Towards baryon-number violation in nuclei from lattice QCD

Michael Wagman

INT Workshop 25-91W

Seattle, WA

January 15, 2025

B-L Violation

BSM sources of *B-L* violation could explain matter-antimatter asymmetry

B-L Violation

BSM sources of *B-L* violation could explain matter-antimatter asymmetry

Dim 5: ***B-L* violating**, *L* violating Majorana neutrino mass

$$\mathcal{L}_5 \sim \left(\frac{1}{\Lambda_{BSM}}\right)(H^T \ell^*)(\bar{\ell} H)$$

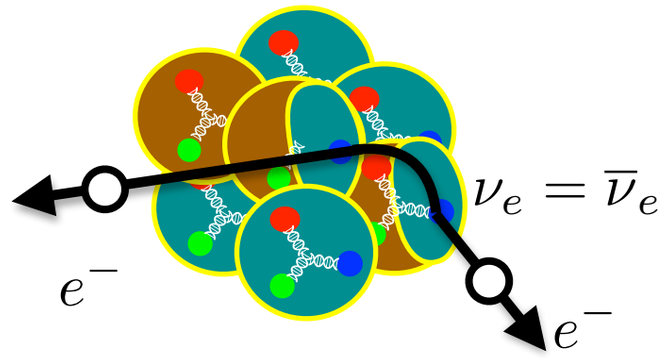

Double-β decay

$\Lambda_{BSM} \gtrsim 10^{10}$ GeV

✓ Leptogenesis

Also dim 7, 9, … see Cirigliano et al JHEP 12 (2018)

B-L Violation

BSM sources of *B-L* violation could explain matter-antimatter asymmetry

Dim 5: ***B-L* violating**, *L* violating Majorana neutrino mass

$$\mathcal{L}_5 \sim \left(\frac{1}{\Lambda_{BSM}}\right)(H^T \ell^*)(\bar{\ell} H)$$

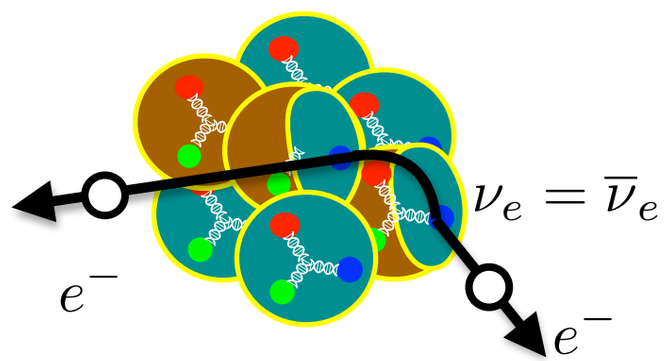

Double-β decay

$\Lambda_{BSM} \gtrsim 10^{10}$ GeV

✓ Leptogenesis

Also dim 7, 9, … see Cirigliano et al JHEP 12 (2018)

Dim 6: ***B-L* conserving**, *B* violating proton decay operators

$$\mathcal{L}_6 \sim \left(\frac{1}{\Lambda^2_{BSM}}\right) uude + \ldots \qquad \pi^0$$

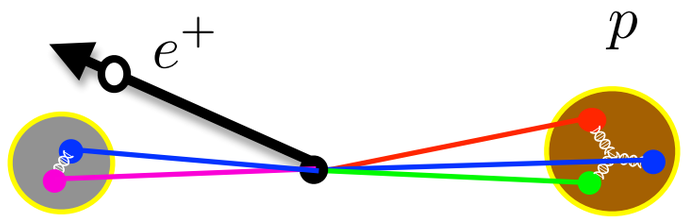

Proton decay

$\Lambda_{BSM} \gtrsim 10^{16}$ GeV

✗ Washed out by sphalerons*

*usually, but see Heeck, Takhistov, PRD 101 (2020)

B-L Violation

BSM sources of *B-L* violation could explain matter-antimatter asymmetry

Dim 5: ***B-L* violating**, *L* violating Majorana neutrino mass

$$\mathcal{L}_5 \sim \left(\frac{1}{\Lambda_{BSM}}\right)(H^T \ell^*)(\bar{\ell} H)$$

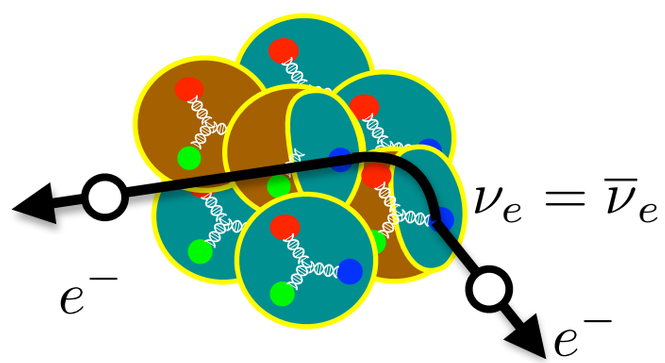

Double-β decay

$\Lambda_{BSM} \gtrsim 10^{10}$ GeV

✓ Leptogenesis

Also dim 7, 9, … see Cirigliano et al JHEP 12 (2018)

Dim 6: ***B-L* conserving**, *B* violating proton decay operators

$$\mathcal{L}_6 \sim \left(\frac{1}{\Lambda^2_{BSM}}\right) uude + \ldots \qquad \pi^0$$

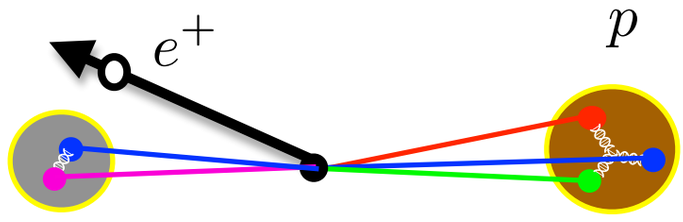

Proton decay

$\Lambda_{BSM} \gtrsim 10^{16}$ GeV

✗ Washed out by sphalerons*

*usually, but see Heeck, Takhistov, PRD 101 (2020)

Dim 9: ***B-L* violating**, *B* violating Majorana neutron mass

$$\mathcal{L}_9 \sim \left(\frac{1}{\Lambda^5_{BSM}}\right) uddudd + \ldots$$

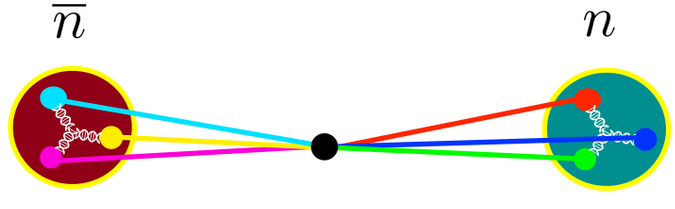

Neutron-antineutron oscillations

$\Lambda_{BSM} \gtrsim 10^5$ GeV

✓ Post-sphaleron baryogengesis

Neutron-Antineutron Oscillations

$n\bar{n}$ oscillation phenomenology similar to meson, neutrino oscillations

$$\mathcal{P}_{n\bar{n}} = \sin^2(t/\tau_{n\bar{n}})e^{-\Gamma_n t} \qquad \tau_{n\bar{n}}^{-1} = \langle \bar{n}|H_9|n\rangle$$

In order to turn experimental constraints into BSM physics constraints, we need theory predictions of $\tau_{n\bar{n}}$ including QCD strong interaction effects

Institut Laue-Langevin (ILL)

$$\tau_{n\bar{n}} > 0.89 \times 10^8 \text{ s}$$

Baldo-Ceolin et al, Zeitschrift für Physik C Particles and Fields (1994)

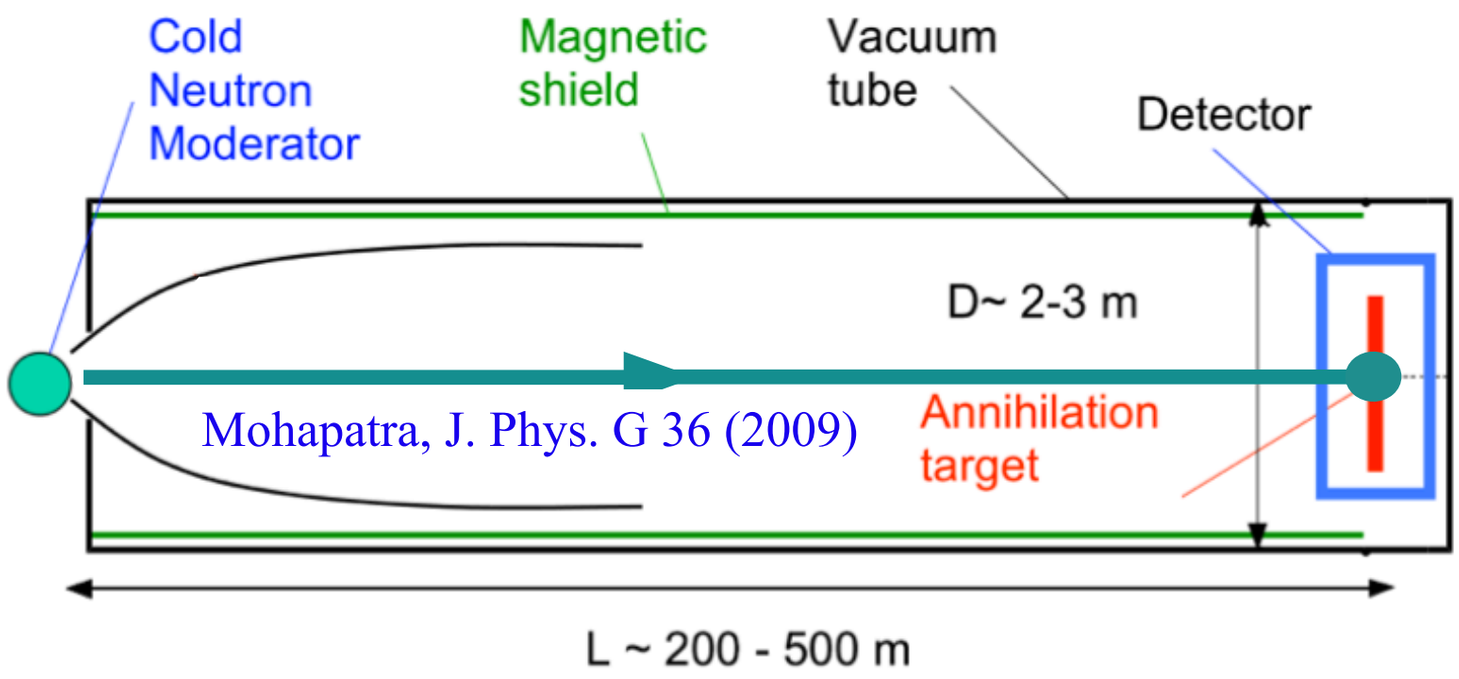

Future experiments at the European Spallation Source could increase sensitivity to $\tau_{n\bar{n}}$ by an order of magnitude

Addazi et al, J. Phys. G. 48 (2021)

$n\bar{n}$ and LQCD

High-scale new physics can be parametrized in SM EFT:

$$\mathcal{L}_9 = \frac{1}{\Lambda_{BSM}^5} \sum_I C_I^{\overline{\rm MS}}(\Lambda_{BSM}) Q_I^{\overline{\rm MS}}(\Lambda_{BSM})$$

Complete basis of six-quark operators

Three-point correlation functions involving Q_I computable in LQCD

$$G_I^{n\overline{n}}(t,\tau) = \int \mathcal{D}\overline{q}\mathcal{D}q\mathcal{D}U e^{-S_{QCD}} \sum_{\mathbf{x},\mathbf{y}} n(\mathbf{x}, t-\tau)\ Q_I^\dagger(0)\ n(\mathbf{y}, -\tau)$$

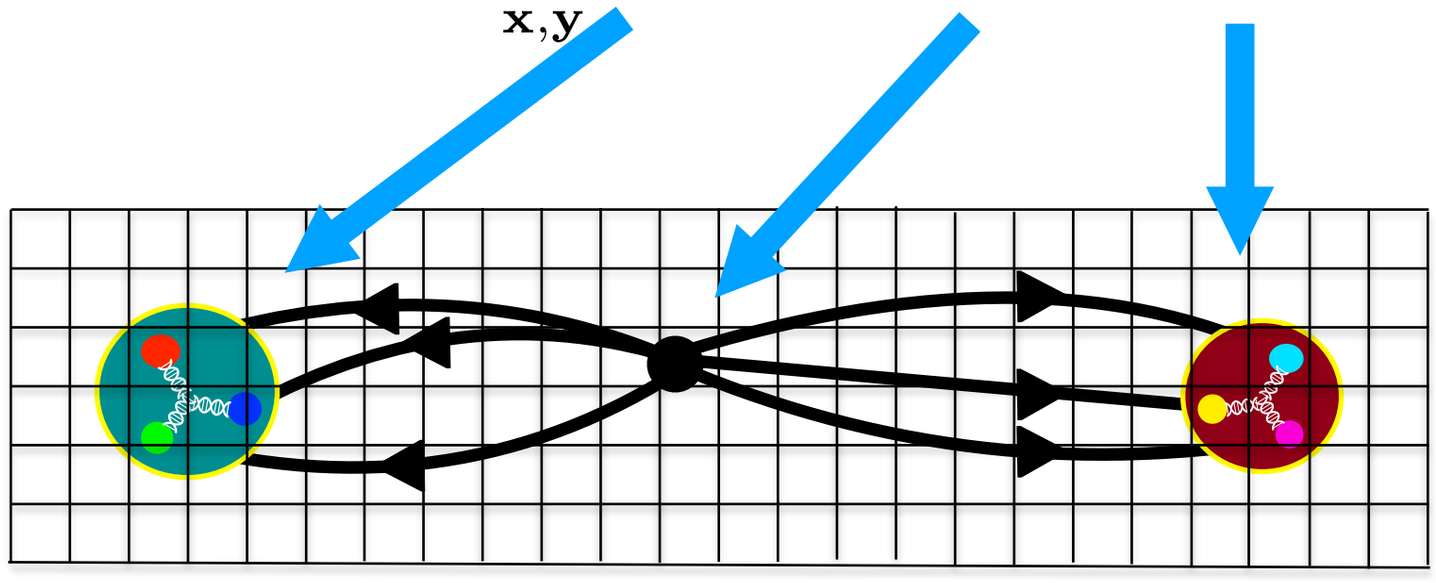

Rinaldi, Sryitsyn, MW et al, PRL 122 (2019); PRD 99 (2019)

Ratio of $n\bar{n}$ and neutron correlation functions gives matrix elements plus excited state effects that can be studied by e.g. two-state fits

Neutron-Antineutron Oscillations

LQCD calculations performed with

✓ ~physical quark masses

✓ nonperturbative renormalization

✗ 1 lattice spacing / volume

FV ChEFT: Bijens and Kofoed, Eur Phys J C (2017)

Rinaldi, Sryitsyn, MW et al, PRL 122 (2019)

	$\mathcal{M}_I^{\overline{\rm MS}}(700\ {\rm TeV})\ [10^{-5}\ {\rm GeV}^6]$
Q_1	$-26(7)$
Q_2	$144(26)$
Q_3	$-47(11)$
Q_5	$-0.23(10)$

Standard Model EFT:

$$\tau_{n\text{-}\overline{n}}^{-1} = \frac{10^{-9}\ \text{s}^{-1}}{(700\ \text{TeV})^{-5}} \left| 4.2(1.1)\widehat{C}_1^{\overline{\rm MS}}(\mu) - 8.6(1.5)\widehat{C}_2^{\overline{\rm MS}}(\mu) + 4.5(1.1)\widehat{C}_3^{\overline{\rm MS}}(\mu) + 0.096(43)\widehat{C}_5^{\overline{\rm MS}}(\mu) \right|_{\mu=2\ \text{GeV}}$$

ILL:

$$\tau_{n\overline{n}} > 0.89 \times 10^8\ \text{s}$$

LR-symmetric example:

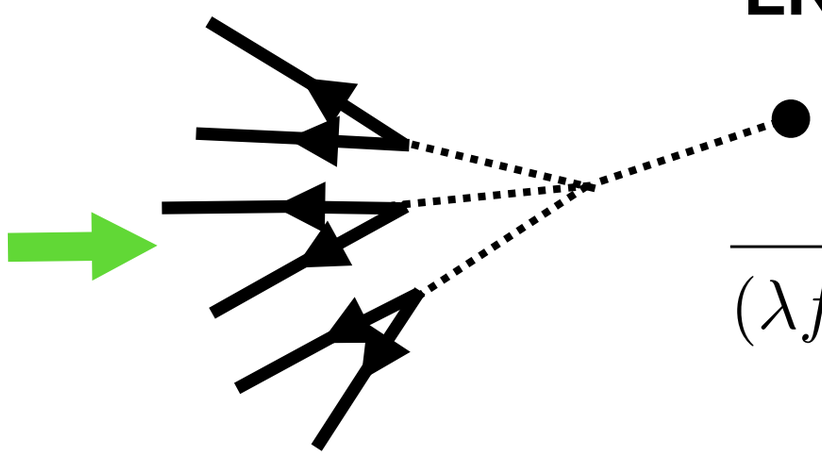

$$\frac{\Lambda_{BSM}}{\left(\lambda f^3 \widetilde{v}_{B-L}\right)^{1/5}} > 390 \pm 22\ \text{TeV}$$

Experimental Implications

Rinaldi, Sryitsyn, MW et al, PRL 122 (2019) Rao, Shrock, Nucl. Phys. B 232 (1984)

	$\mathcal{M}_I^{\overline{\rm MS}}(700\ {\rm TeV})\ [10^{-5}\ {\rm GeV}^6]$	MIT Bag $\times$ RG $[10^{-5}\ {\rm GeV}^6]$
Q_1	$-26(7)$	$-6.4,\ -5.2$
Q_2	$144(26)$	$16,\ 19$
Q_3	$-47(11)$	$-9.1,\ -7.6$
Q_5	$-0.23(10)$	$-0.28,\ 0.15$

For fixed BSM parameters, QCD predicts experimental sensitivity is **25 - 64 times higher** than predicted using MIT bag model

$$N_{events} \propto \tau_{n\overline{n}}^{-2} \approx \left(\sum_{I=1}^{3} \widehat{C}_I^{\overline{\rm MS}}(\Lambda_{BSM}) \mathcal{M}_I^{\overline{\rm MS}}(\Lambda_{BSM}) \right)^2$$

For $SU(2)_L \times SU(2)_R \times SU(4)_C$ example, lower bound on BSM couplings from ILL **390 TeV** instead of **290 TeV**

Butkeia, Sigiel, PRD 97 (2018)

B violation in nuclei

Future large-volume detectors such as DUNE and Hyper-Kamiokande will provide new discoveries or limits of intranuclear neutron-antineutron oscillations ($n\bar{n}$)

Getting from experiments involving nuclei to constraints on BSM requires theory:

- Nuclear models (error bars?)
- Direct LQCD calculations (computation?)
- **LQCD informed hadronic and nuclear effective theories**

Intranuclear $n\bar{n}$ simulation

Abratenko et al [MicroBooNE] JINST 19 (2024)

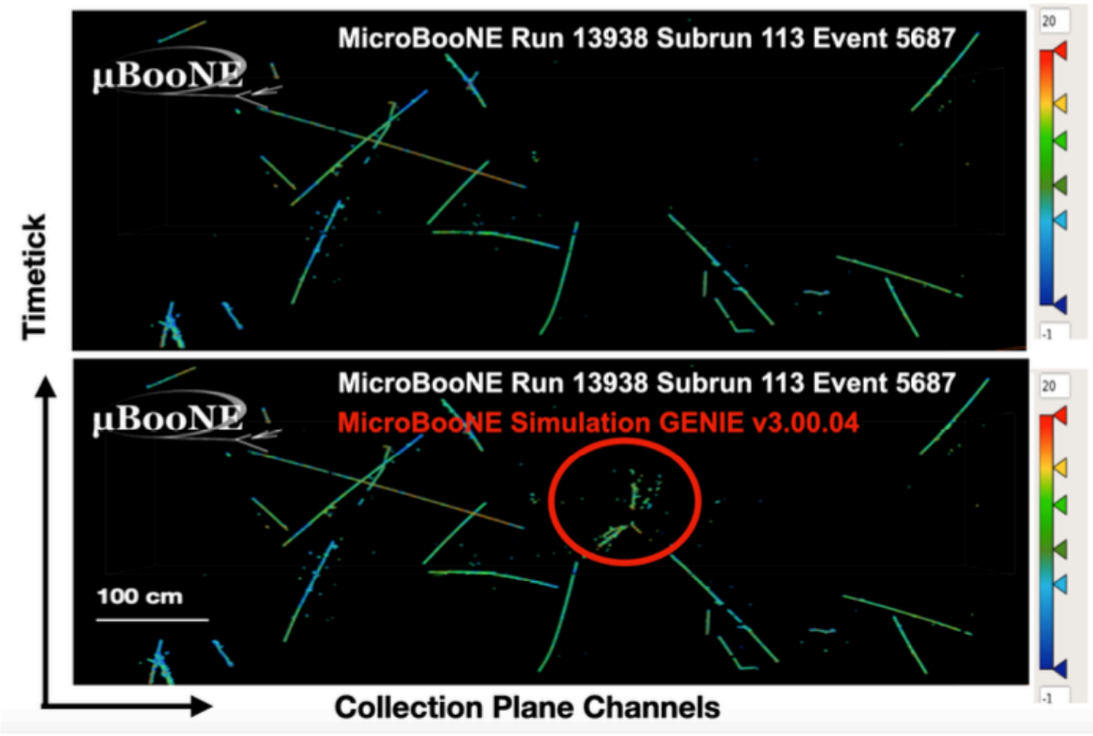

DUNE

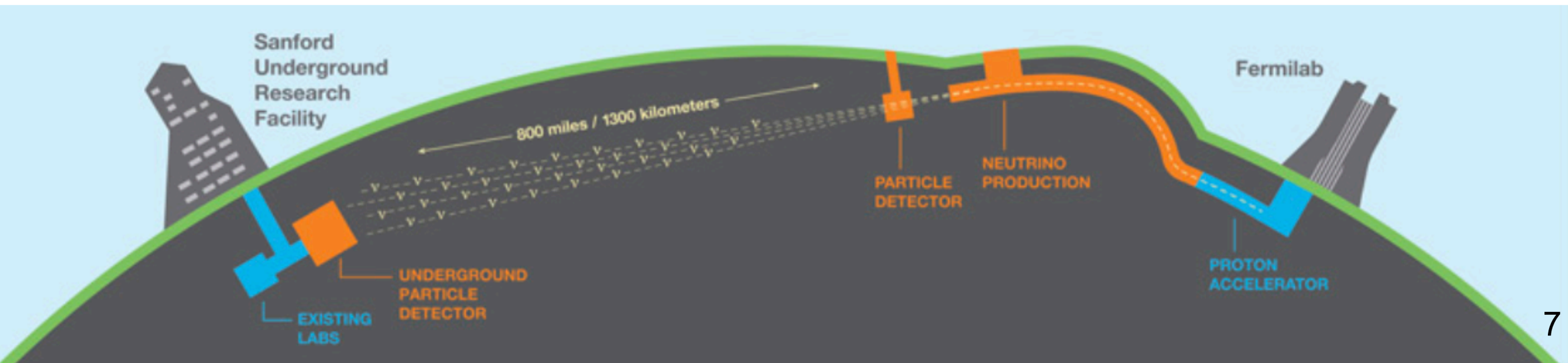

$n\bar{n}$ in nuclei

Deuteron lifetime related to $\tau_{n\bar{n}}$ in chiral EFT

….but results sensitive to choice of power counting

See talk by Bira van Kolck yesterday

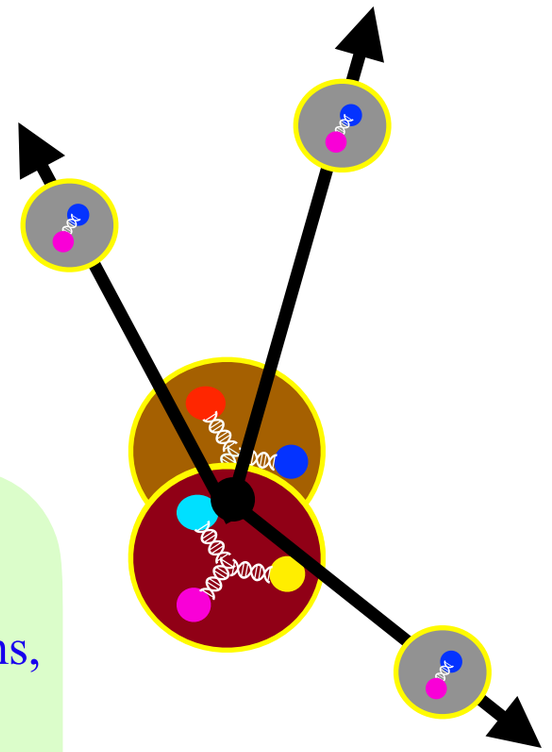

SNO constraint:

$\Gamma_d^{-1} > 1.18 \times 10^{31}$ years

Aharmin et al [SNO], PRD 96 (2017)

KSW

$\tau_{n\bar{n}} > 1.6 \times 10^8$ s

Oosterhof, Long, de Vries, Timmermans, van Kolck, PRL 122 (2019)

$\tau_{n\bar{n}} > 2.6 \times 10^8$ s

Weinberg

Haidenbauer and Meißner, Chinese Physics C 44 (2020)

Oxygen lifetime provides possibly stronger but more uncertain constraints

Super K constraint

$\Gamma_{O^{16}}^{-1} > 19 \times 10^{31}$ years

Abe et al [Super K], PRD 91 (2015)

$\tau_{n\bar{n}} \gtrsim 2.7 \times 10^8$ s

State-of-the-art optical potentials:

Friedman, Gal, PRD 78 (2008)

Dineutron decay with LQCD

Future argon lifetime constraints from DUNE will be even more challenging to analyze — can LQCD help benchmark the two-nucleon sector?

Simplest possible lattice QCD calculation of $n\overline{n}$ in multi-nucleon system:

$$\left\langle Q_I(t) n n^\dagger(0) \right\rangle \quad =$$

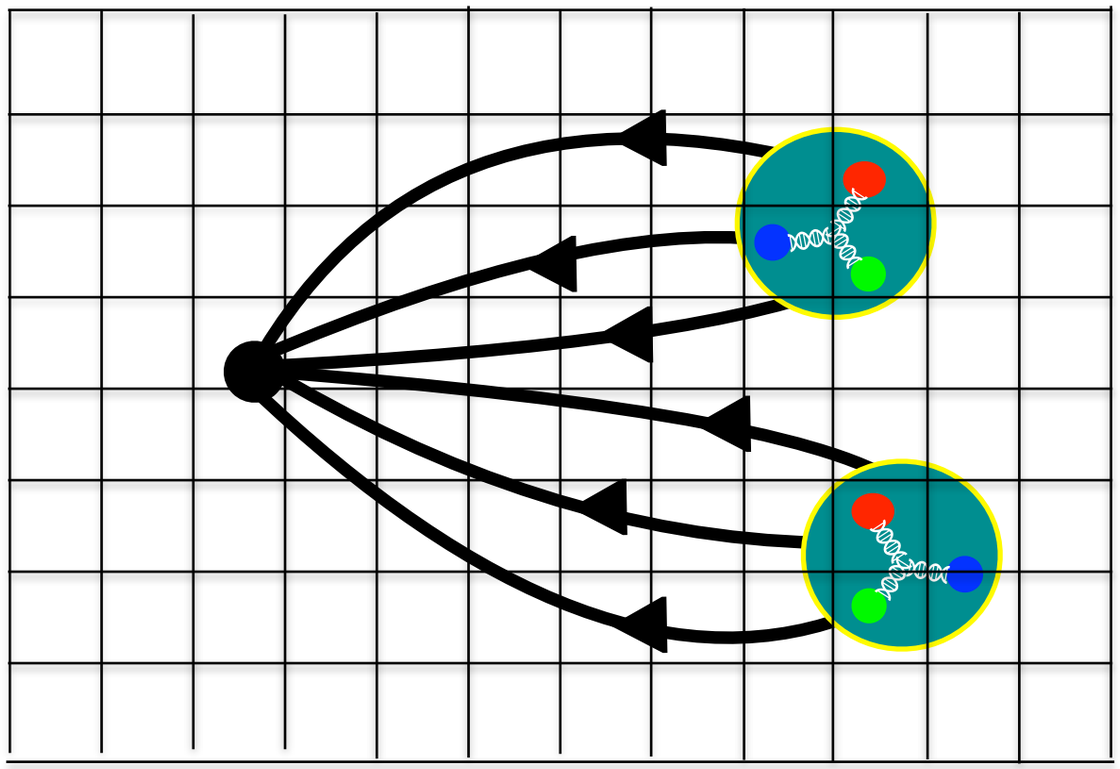

Dineutron decay matrix element can be extracted from LQCD two-point function

$$\left\langle Q_I(t) n n^\dagger(0) \right\rangle \sim \sum_J \langle 0|Q_J|nn\rangle \, Z_{JI} + \ldots$$

Nonperturbative QCD matrix element contains info to constrain unknown NLO+ EFT couplings that may have sizable impact even on deuterium

Oosterhof et al, PRL 122 (2019) Haidenbauer and Meißner, Chinese Physics C 44 (2020)

$n\bar{n}$ and crossing symmetry

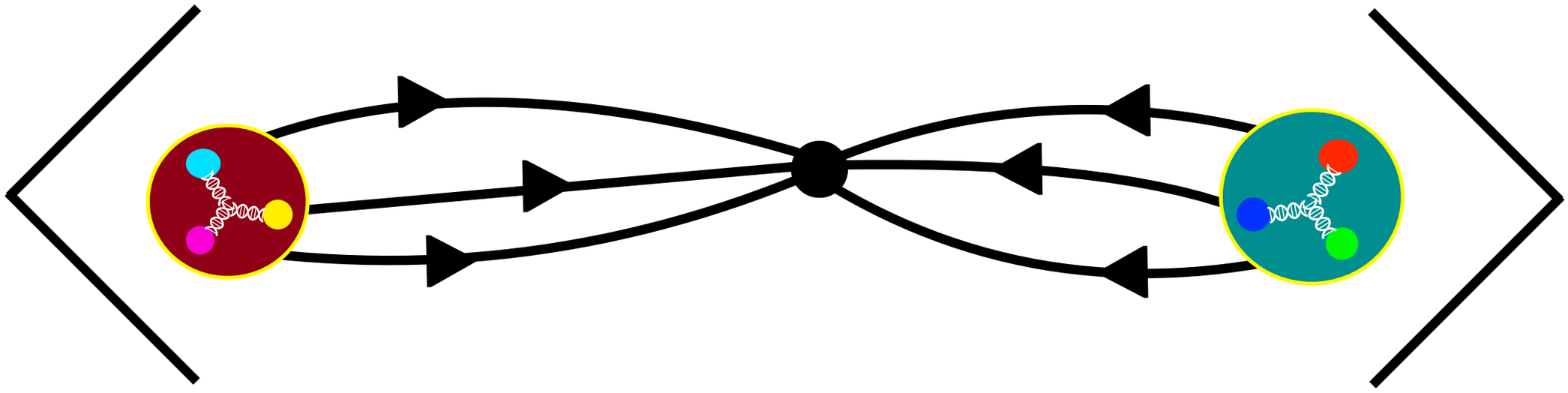

?

=

Crossing symmetry

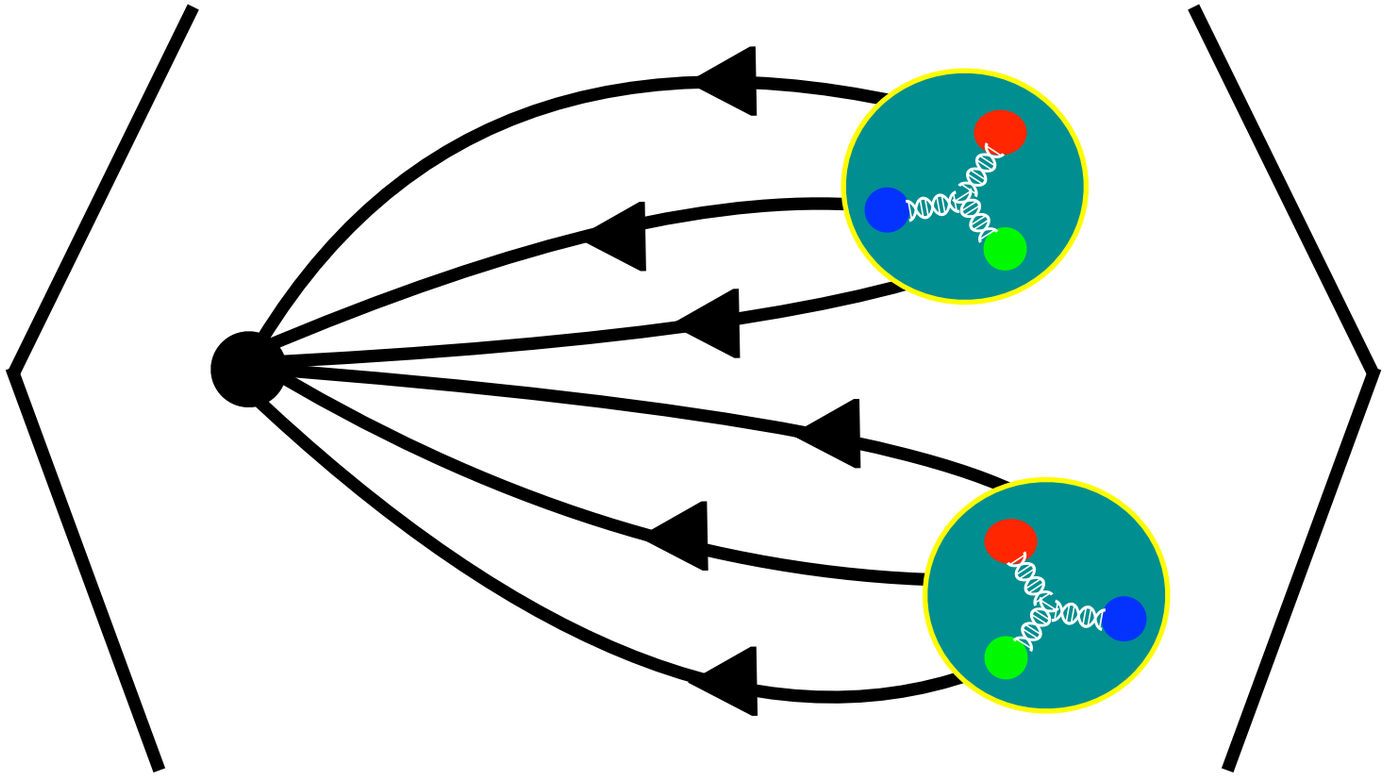

$n\bar{n}$ and crossing symmetry

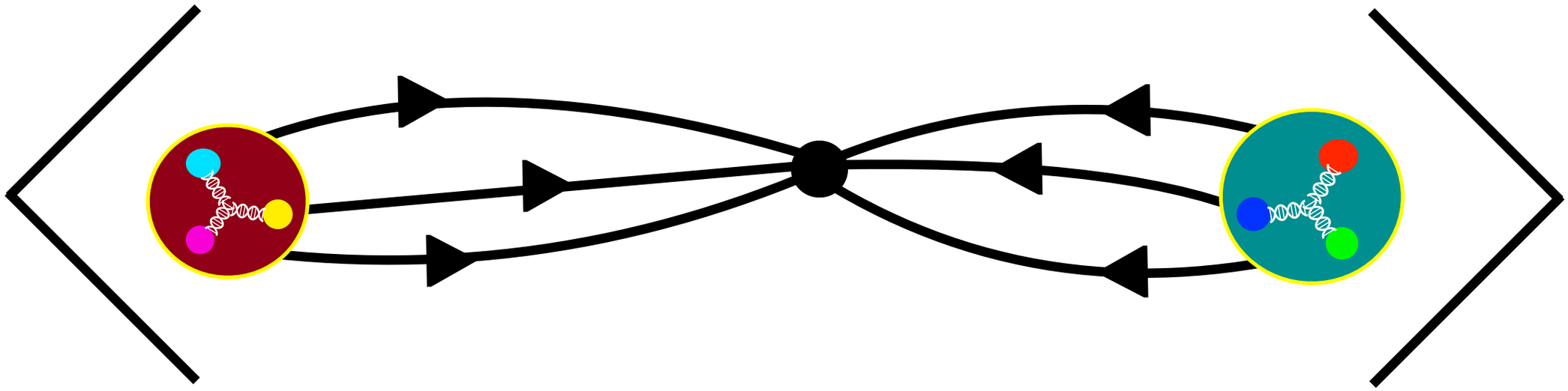

Crossing valid for scattering amplitudes not matrix elements

Crossing symmetry

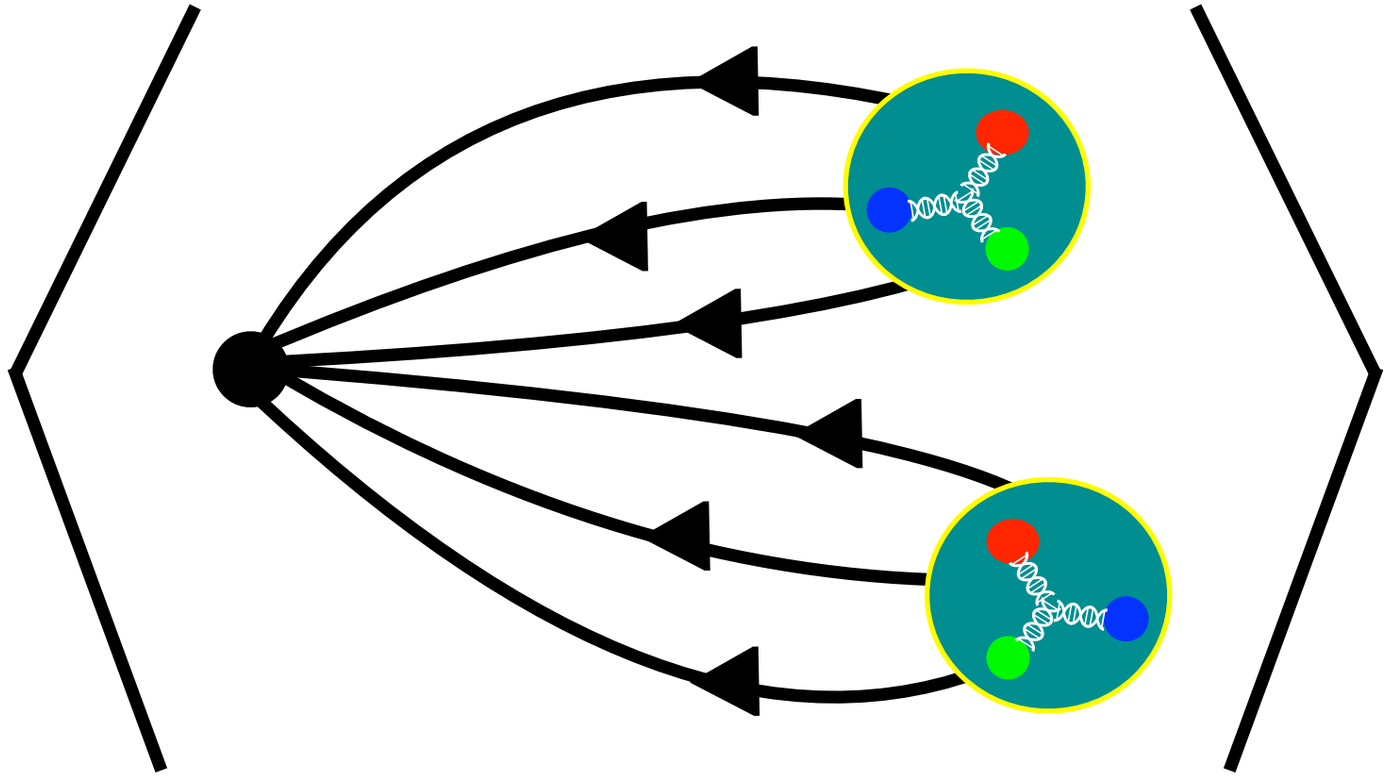

$n\bar{n}$ and crossing symmetry

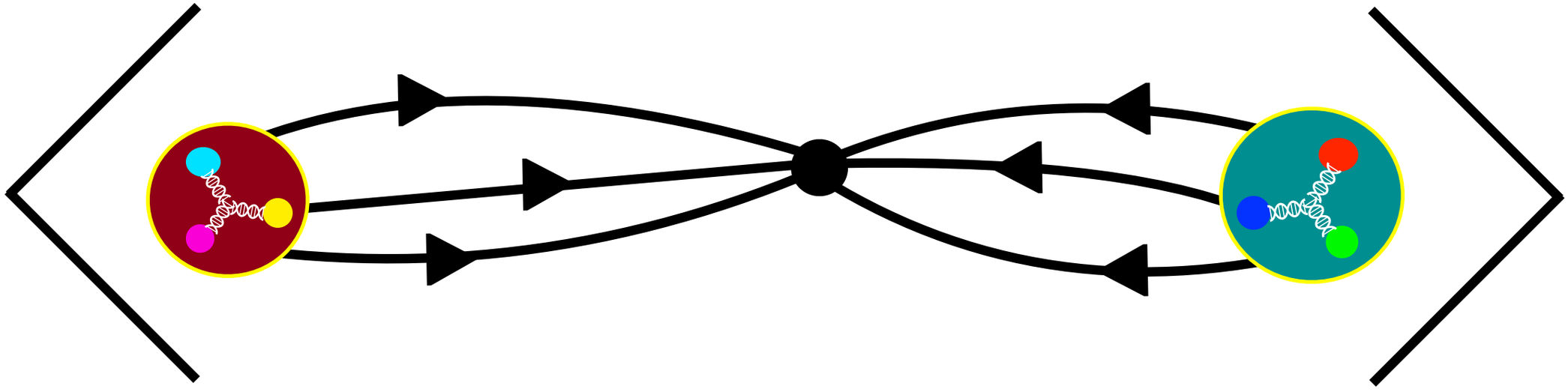

Crossing valid for scattering amplitudes not matrix elements

=

Crossing symmetry

$$2M_N \left\langle \right.$$

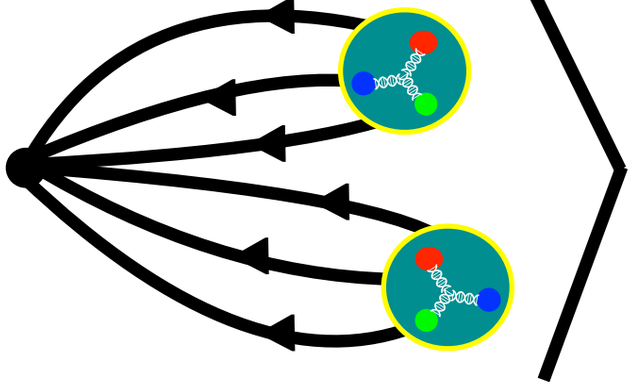

$$\left. \right\rangle$$

$$\sqrt{\left\langle \right.}$$

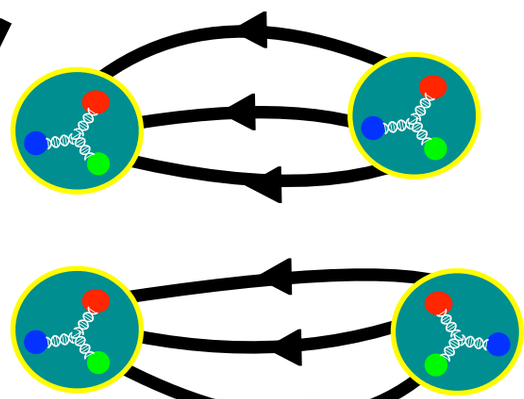

$$\left. \right\rangle$$

Towards $n\bar{n}$ in nuclei

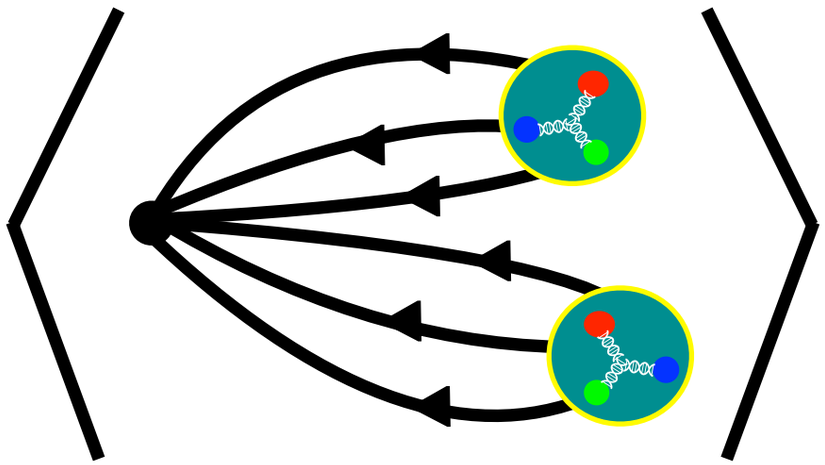

=

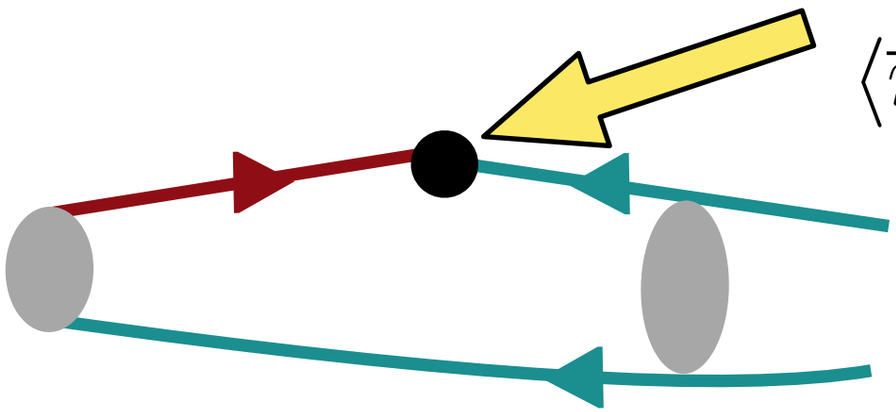

"Known"
EFT input
$\langle \overline{n} | Q_I | n \rangle$

Dineutron decay matrix elements
can be matched to nuclear EFTs
to constrain higher-order LECs

Nuclear EFT

- Nucleon propagator
- Antinucleon propagator
- Strong interactions (resummed)

+

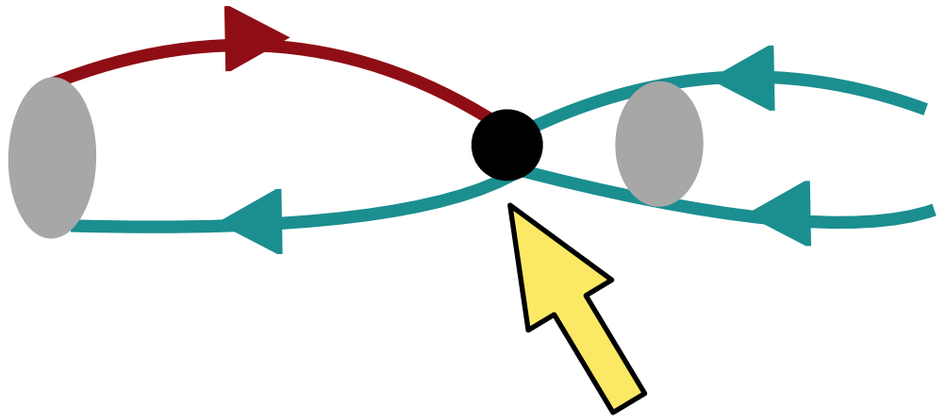

Unknown EFT input

$\langle n\overline{n} | Q_I | nn \rangle$

+ . . .

~ NLO input discussed in

Oosterhof et al, PRL 122 (2019)

LQCD and $n\bar{n}$ in nuclei

LQCD calculations can use the same codes (and some data)
as NN spectroscopy calculations using correlator matrices

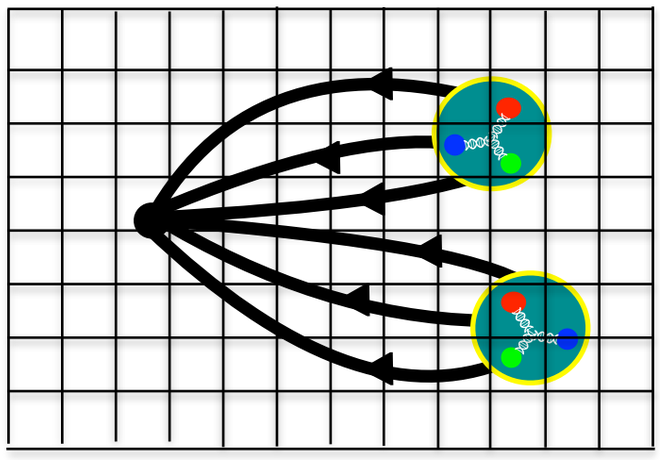

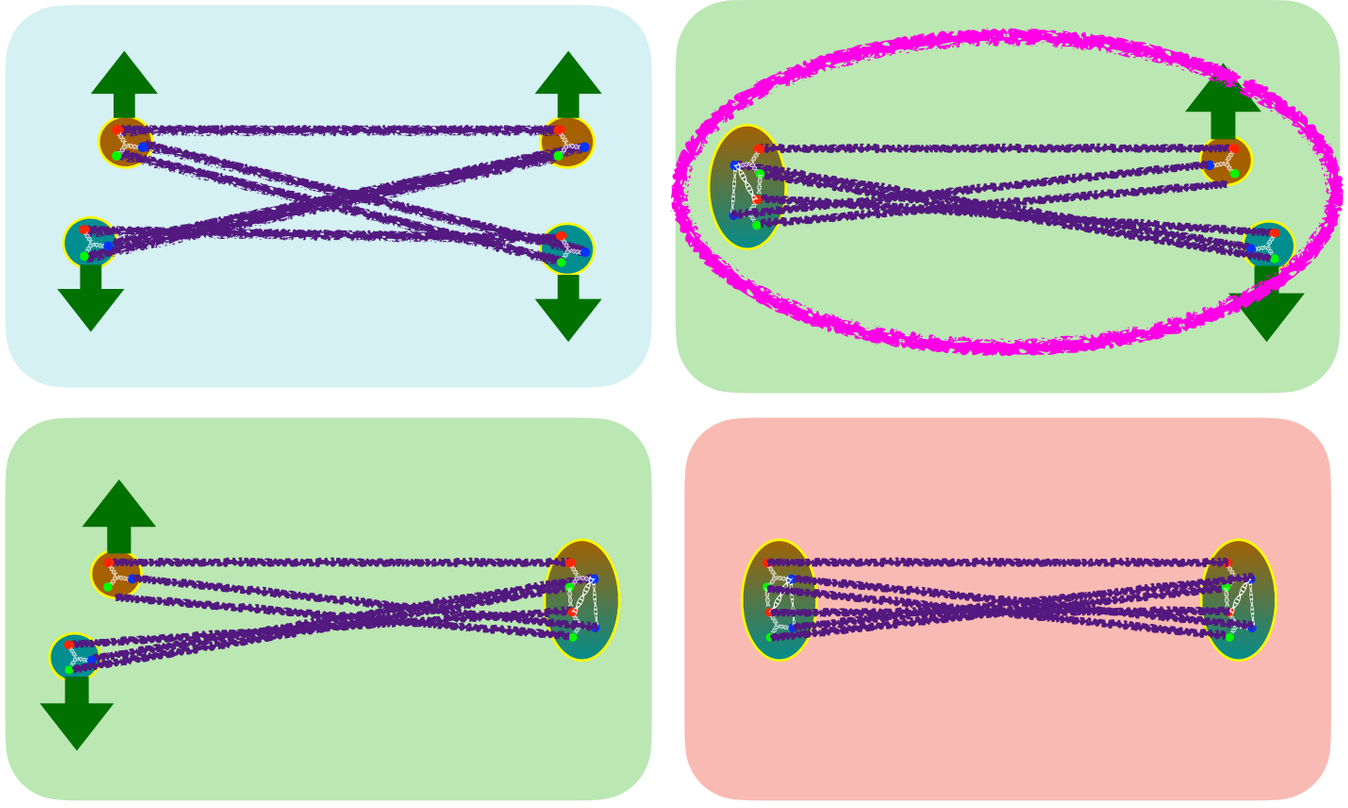

Correlator topology
corresponds to
“hexaquark” - “dibaryon”
off-diagonal element of
correlator matrix

Amarasinghe, MW et al [NPLQCD], PRD 107 (2023)

MW, *PoS* LATTICE2021

Nicholson et al, *PoS* LATTICE2021

Detmold, Perry, MW et al [NPLQCD], arXiv:2404.12039

nn wavefunction catalog

Detmold, Perry, MW et al [NPLQCD], arXiv:2404.12039

- Complete bases of local hexaquark operators with deuteron and dineutron quantum numbers

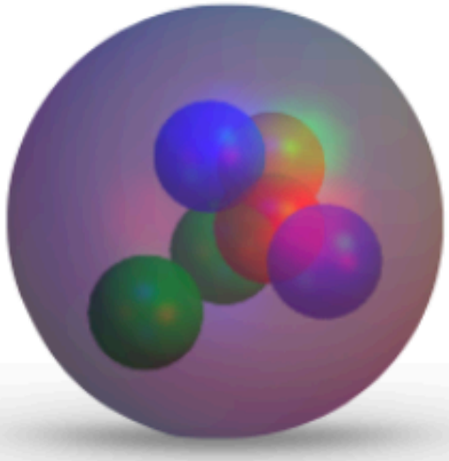

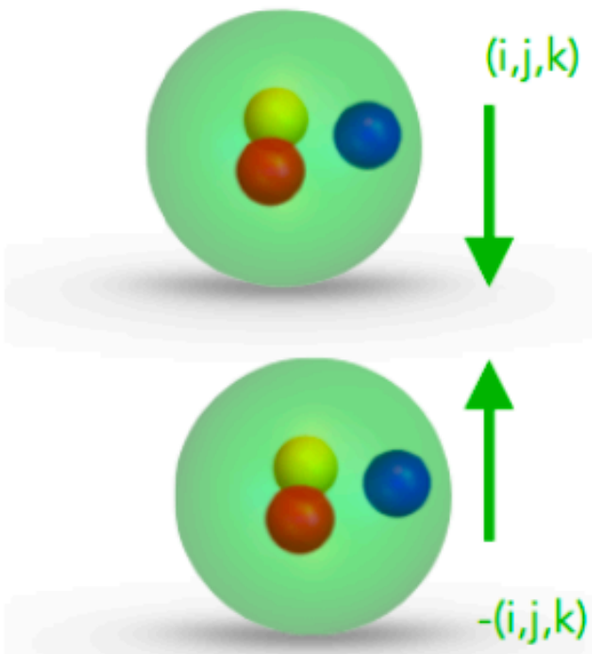

- Plane-wave dibaryon operators including all spinor components*

- Exponentially correlated quasi-local operators including all spinor components*

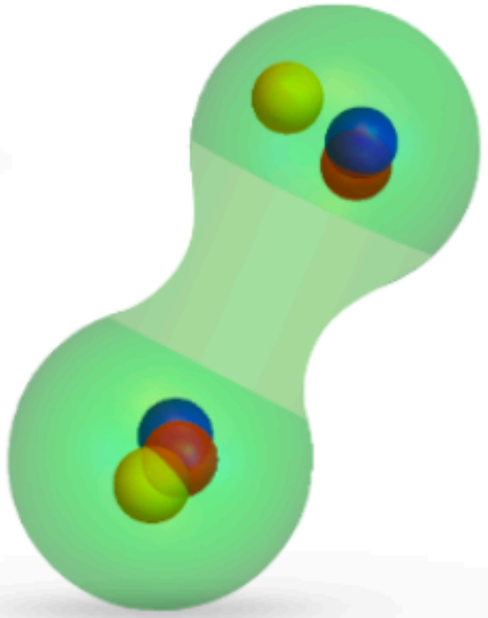

*previous study used only the Dirac basis upper components arising in nonrelativistic quark models

Constructing a hexaquark basis

Hexaquark construction simplified by introducing “diquarks”

$$\mathcal{D}^{ab}_{\Gamma,F}(x) = \frac{1}{\sqrt{2}} q^{aT}(x) C\Gamma i\tau_2 F q^b(x)$$

Dirac spinor matrix

SU(2) isospin flavor matrix

$$\mathcal{H}^K(x) = \mathcal{H}^{C_1C_2C_3}_{\Gamma_1,F_1;\Gamma_2,F_2;\Gamma_3,F_3}(x)$$

$$= T^{C_1C_2C_3}_{abcdef} \mathcal{D}^{ab}_{\Gamma_1,F_1}(x) \mathcal{D}^{cd}_{\Gamma_2,F_2}(x) \mathcal{D}^{ef}_{\Gamma_3,F_3}(x)$$

Color state is product of three symmetric ($\mathbf{6}$) or antisymmetric ($\mathbf{3}$) diquarks

$$(\mathbf{3}\otimes\mathbf{3})\otimes(\mathbf{3}\otimes\mathbf{3})\otimes(\mathbf{3}\otimes\mathbf{3}) = (\mathbf{6}\oplus\overline{\mathbf{3}})\otimes(\mathbf{6}\oplus\overline{\mathbf{3}})\otimes(\mathbf{6}\oplus\overline{\mathbf{3}})$$

Constructing a hexaquark basis

Hexaquark construction simplified by introducing “diquarks”

$$\mathcal{D}^{ab}_{\Gamma,F}(x) = \frac{1}{\sqrt{2}} q^{aT}(x) C\Gamma i\tau_2 F q^b(x)$$

Dirac spinor matrix

SU(2) isospin flavor matrix

$$\mathcal{H}^K(x) = \mathcal{H}^{C_1C_2C_3}_{\Gamma_1,F_1;\Gamma_2,F_2;\Gamma_3,F_3}(x)$$

$$= T^{C_1C_2C_3}_{abcdef} \mathcal{D}^{ab}_{\Gamma_1,F_1}(x) \mathcal{D}^{cd}_{\Gamma_2,F_2}(x) \mathcal{D}^{ef}_{\Gamma_3,F_3}(x)$$

Color state is product of three symmetric ($\mathbf{6}$) or antisymmetric ($\mathbf{3}$) diquarks

$$(\mathbf{3}\otimes\mathbf{3})\otimes(\mathbf{3}\otimes\mathbf{3})\otimes(\mathbf{3}\otimes\mathbf{3}) = (\mathbf{6}\oplus\overline{\mathbf{3}})\otimes(\mathbf{6}\oplus\overline{\mathbf{3}})\otimes(\mathbf{6}\oplus\overline{\mathbf{3}})$$

Five ways to form singlets from diquark products

$$\overline{\mathbf{3}}\otimes\overline{\mathbf{3}}\otimes\overline{\mathbf{3}}\,, \quad \overline{\mathbf{3}}\otimes\overline{\mathbf{3}}\otimes\mathbf{6}\,, \quad \overline{\mathbf{3}}\otimes\mathbf{6}\otimes\overline{\mathbf{3}}\,, \quad \mathbf{6}\otimes\overline{\mathbf{3}}\otimes\overline{\mathbf{3}}\,, \quad \mathbf{6}\otimes\mathbf{6}\otimes\mathbf{6}$$

Five linearly independent color-singlet 6 index tenors Rao and Shrock, Phys. Lett. B 116 (1982)

$$T^{AAA}_{abcdef} = \epsilon_{abe}\epsilon_{cdf} - \epsilon_{abf}\epsilon_{cde}\,, \quad T^{ASA}_{abcdef} = \epsilon_{abc}\epsilon_{efd} + \epsilon_{abd}\epsilon_{efc}\,, \quad T^{SSS}_{abcdef} = \epsilon_{ace}\epsilon_{bdf} + \epsilon_{acf}\epsilon_{bde} + \epsilon_{bce}\epsilon_{adf} + \epsilon_{bcf}\epsilon_{ade}$$

$$T^{AAS}_{abcdef} = \epsilon_{abe}\epsilon_{cdf} + \epsilon_{abf}\epsilon_{cde}\,, \quad T^{SAA}_{abcdef} = \epsilon_{efa}\epsilon_{cdb} + \epsilon_{efb}\epsilon_{cda}\,,$$

A complete hexaquark basis

$$\mathcal{H}^K(x) = \mathcal{H}^{C_1C_2C_3}_{\Gamma_1,F_1;\Gamma_2,F_2;\Gamma_3,F_3}(x) = T^{C_1C_2C_3}_{abcdef}\mathcal{D}^{ab}_{\Gamma_1,F_1}(x)\mathcal{D}^{cd}_{\Gamma_2,F_2}(x)\mathcal{D}^{ef}_{\Gamma_3,F_3}(x)$$

Combined spin-color-flavor Fierz identities complicate identification of linearly independent 6-quark operators

Rao and Shrock, Phys. Lett. B 116 (1982)
Buchoff and MW, PRD 93 (2016)

Out of 5 x 32 x 9 = 1400 color-spin-flavor operator products with dineutron quantum numbers, only **16** are linearly independent after accounting for quark antisymmetry

Detmold, Perry, MW et al [NPLQCD], arXiv:2404.12039

K	Color	Spin			Flavor	K	Color	Spin			Flavor
1	AAA	γ_4	$\gamma_5 P_+$	1	$\tau\ 1\ 1$	9	SAA	$\gamma_5 P_-$	$\gamma_5 P_+$	$\gamma_5 P_+$	$\tau\ 1\ 1$
2	AAA	γ_4	$\gamma_5 P_-$	1	$\tau\ 1\ 1$	10	SAA	$\gamma_5 P_-$	$\gamma_5 P_-$	$\gamma_5 P_+$	$\tau\ 1\ 1$
3	SAA	$\gamma_5 P_+$	$\gamma_5 P_+$	$\gamma_5 P_+$	$\tau\ 1\ 1$	11	SAA	$\gamma_5 P_-$	$\gamma_5 P_-$	$\gamma_5 P_-$	$\tau\ 1\ 1$
4	SAA	$\gamma_5 P_+$	$\gamma_5 P_-$	$\gamma_5 P_+$	$\tau\ 1\ 1$	12	SAA	$\gamma_5 P_-$	1	1	$\tau\ 1\ 1$
5	SAA	$\gamma_5 P_+$	$\gamma_5 P_-$	$\gamma_5 P_-$	$\tau\ 1\ 1$	13	SAA	$\gamma_5 P_-$	γ_4	γ_4	$\tau'\tau\ \tau'$
6	SAA	$\gamma_5 P_+$	1	1	$\tau\ 1\ 1$	14	SAA	$\gamma_5 P_-$	γ_4	γ_4	$\tau\ \tau'\tau'$
7	SAA	$\gamma_5 P_+$	γ_4	γ_4	$\tau'\tau\ \tau'$	15	SSS	$\gamma_5 P_+$	$\gamma_5 P_-$	$\gamma_5 P_+$	$\tau\ \tau'\tau'$
8	SAA	$\gamma_5 P_+$	γ_4	γ_4	$\tau\ \tau'\tau'$	16	SSS	$\gamma_5 P_+$	$\gamma_5 P_-$	$\gamma_5 P_-$	$\tau'\tau\ \tau'$

One operator (#3) is a product of color-singlet baryons, all others involve “hidden color” states not describable by color-singlet products

Harvey, Nucl. Phys. A 352 (1981)

Hidden-color nn states

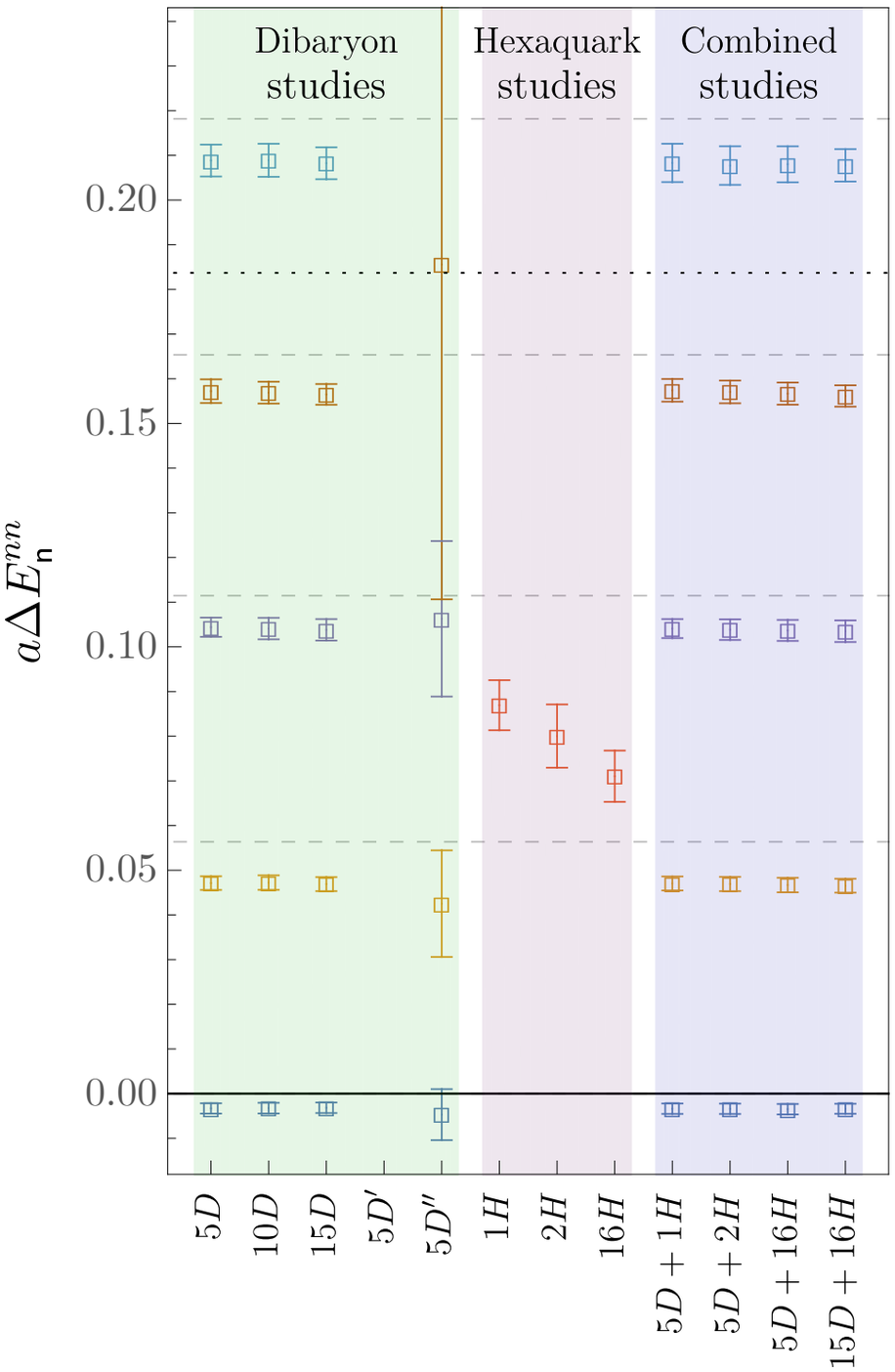

Hidden-color hexaquark and lower-spin-component dibaryon operators do not significantly affect low-energy spectrum

- Hidden-color hexaquarks overlap predominantly with particular excited states that may have novel structure

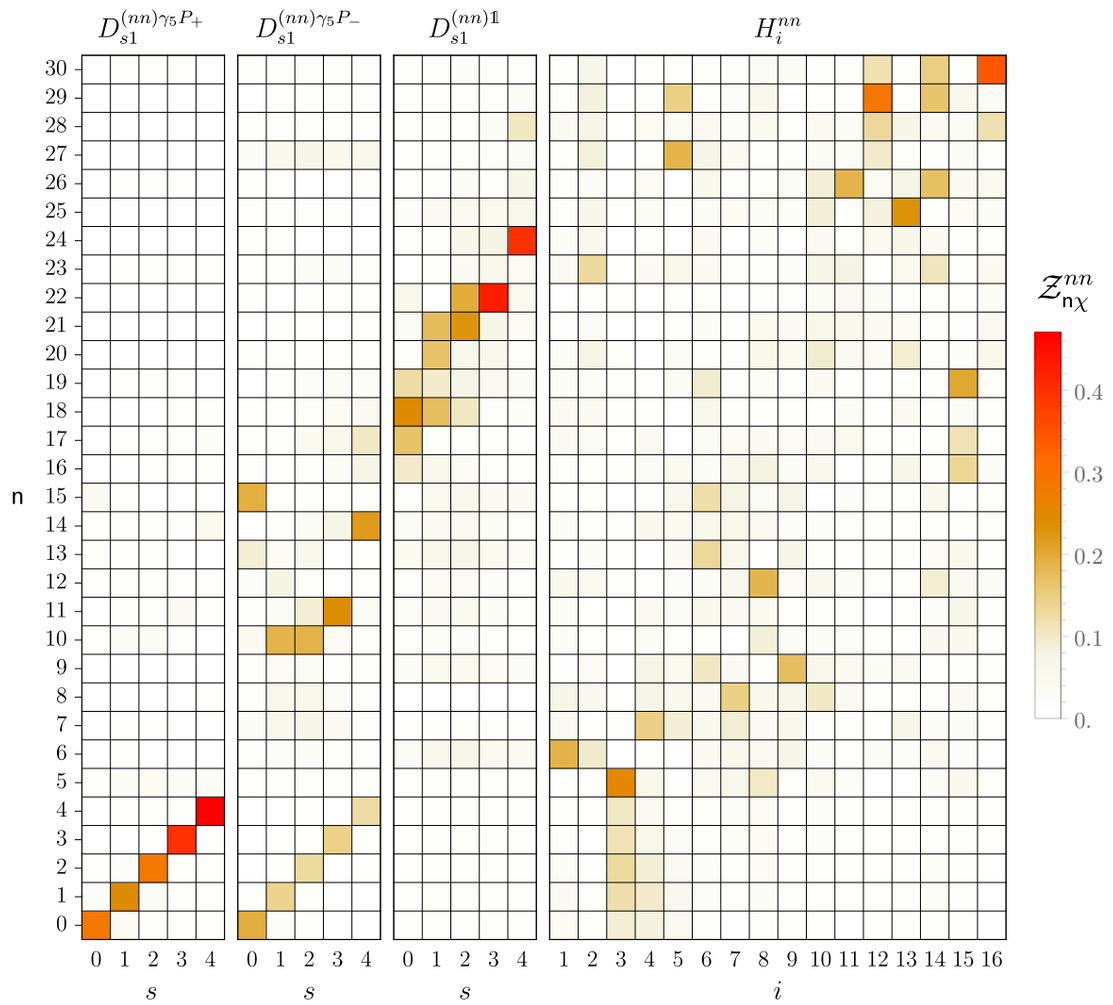

Detmold, Perry, MW et al [NPLQCD], arXiv:2404.12039

LQCD nn decay results

Overlap factors encode ground- and excited-state dineutron decay matrix elements of interest

$$\mathcal{Z}_{\mathsf{n}H_i^{nn}} = \langle 0|H_i^{nn}|nn,\mathsf{n}\rangle$$

$$= \sum_J \langle 0|Q_J|nn,\mathsf{n}\rangle\, C_{Ji}$$

Known change-of-basis matrix

Detmold, Perry, MW et al [NPLQCD], arXiv:2404.12039

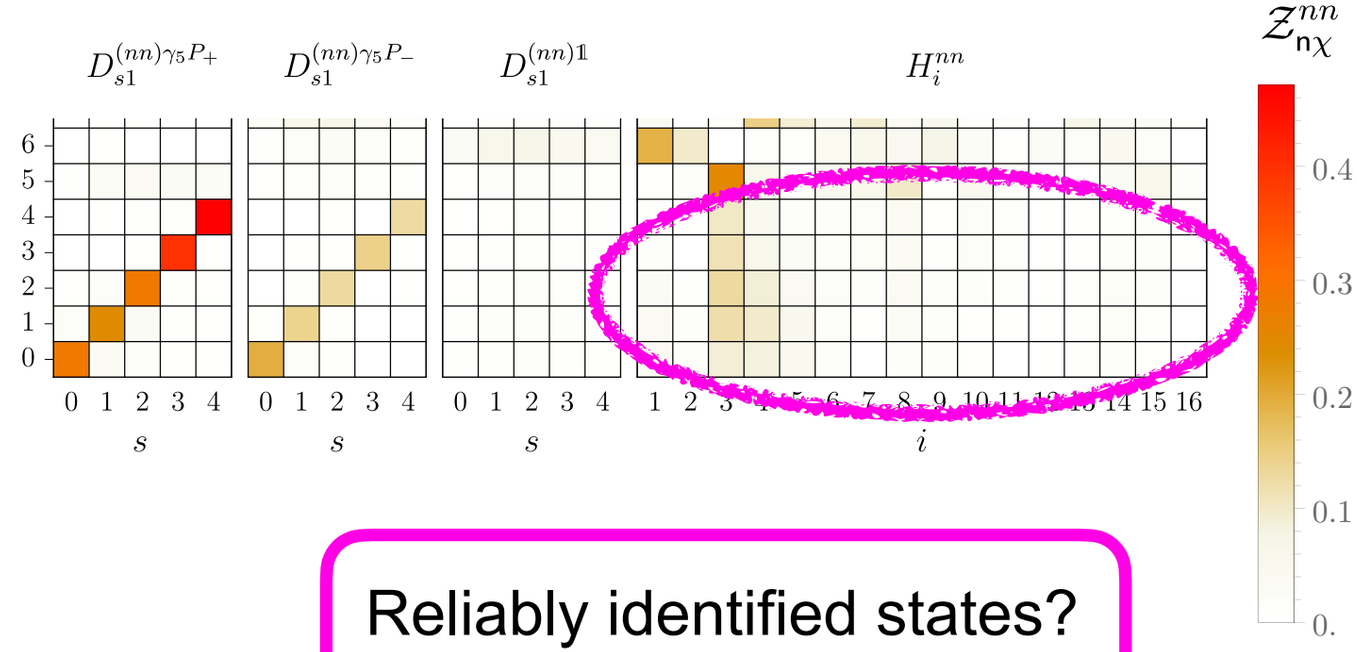

Reliably identified states?

LQCD nn decay results

Overlap factors encode ground- and excited-state dineutron decay matrix elements of interest

$$\mathcal{Z}_{\mathsf{n}H_i^{nn}} = \langle 0|H_i^{nn}|nn,\mathsf{n}\rangle$$

$$= \sum_J \langle 0|Q_J|nn,\mathsf{n}\rangle\, C_{Ji}$$

Known change-of-basis matrix

Detmold, Perry, MW et al [NPLQCD], arXiv:2404.12039

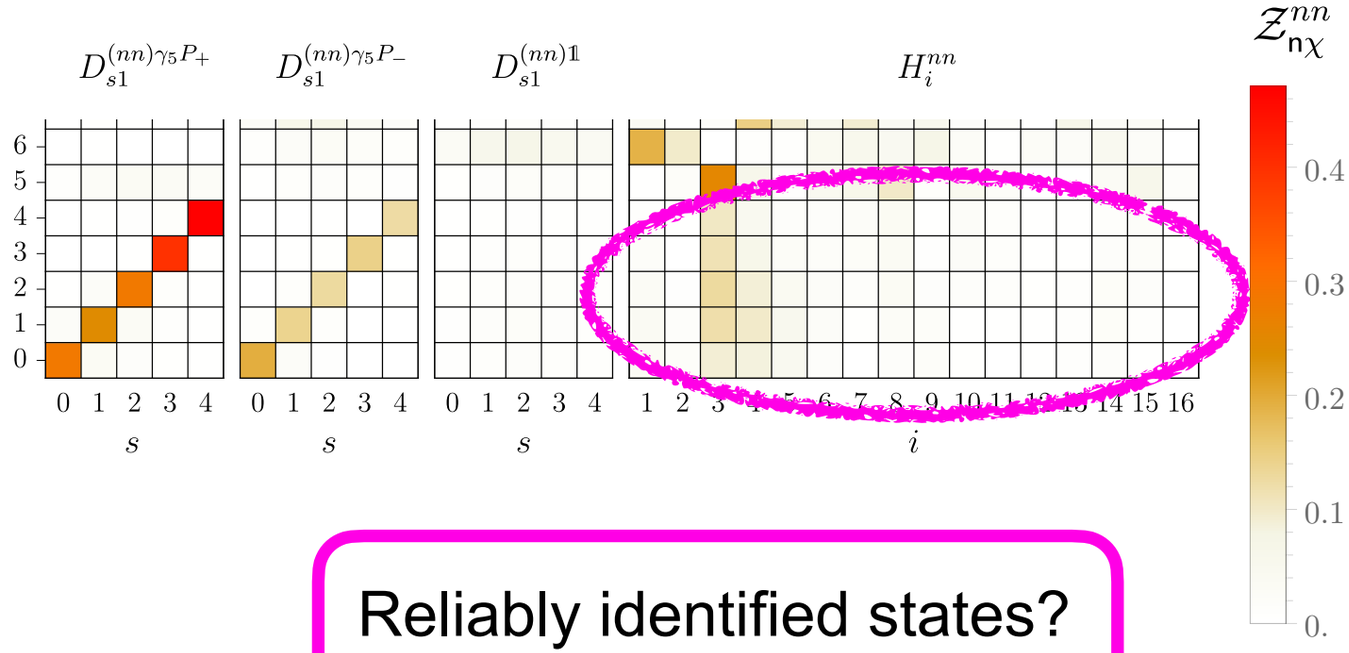

Reliably identified states?

Qualitative lessons

- Strong energy (i.e. state n) dependence of $\langle 0|H_i^{nn}|nn,\mathsf{n}\rangle$ suggests nuclear matrix elements sensitive to neutron (pair) distribution inside nucleus

LQCD nn decay results

Overlap factors encode ground- and excited-state dineutron decay matrix elements of interest

$$\mathcal{Z}_{\mathsf{n}H_i^{nn}} = \langle 0|H_i^{nn}|nn,\mathsf{n}\rangle$$

$$= \sum_J \langle 0|Q_J|nn,\mathsf{n}\rangle\, C_{Ji}$$

Known change-of-basis matrix

Detmold, Perry, MW et al [NPLQCD], arXiv:2404.12039

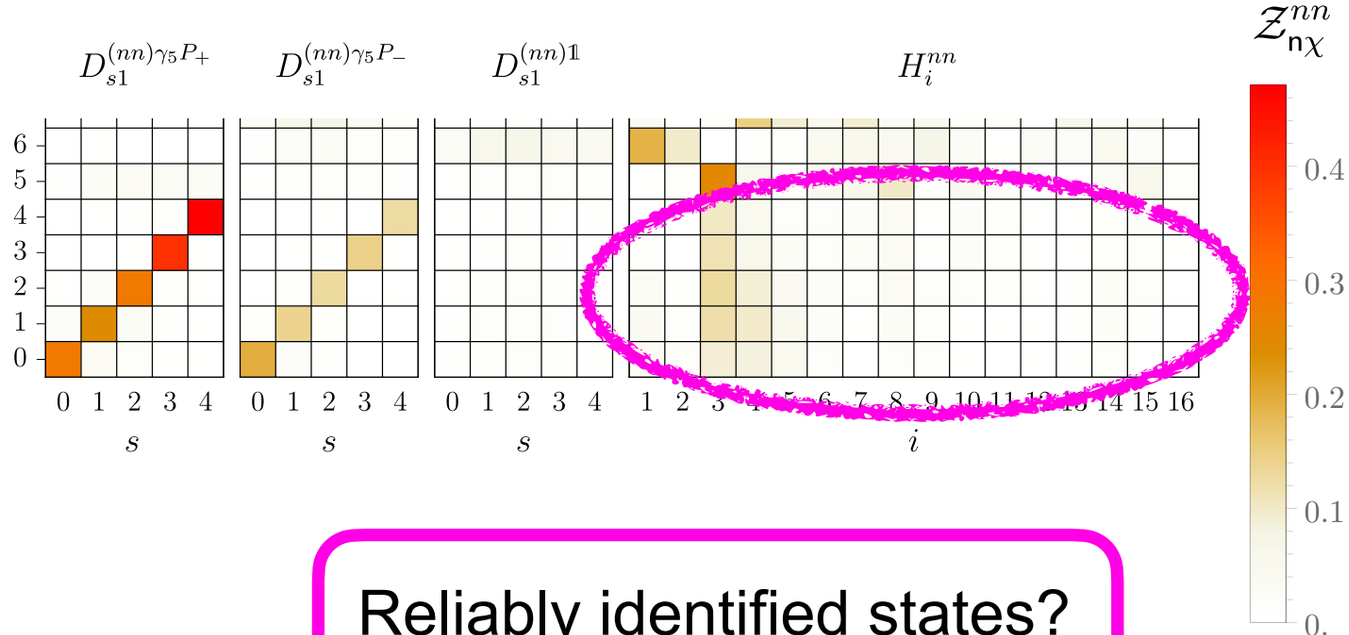

Reliably identified states?

Qualitative lessons

- Strong energy (i.e. state n) dependence of $\langle 0|H_i^{nn}|nn,\mathsf{n}\rangle$ suggests nuclear matrix elements sensitive to neutron (pair) distribution inside nucleus

Quantitative challenges remain

- Nonperturbative renormalization complicated (need NPR for this action, smeared- vs point-like)
- Challenging to estimate systematic uncertainties associated with state identification…

Variational bounds

Variational upper bounds obtained using different interpolating operator sets are consistent

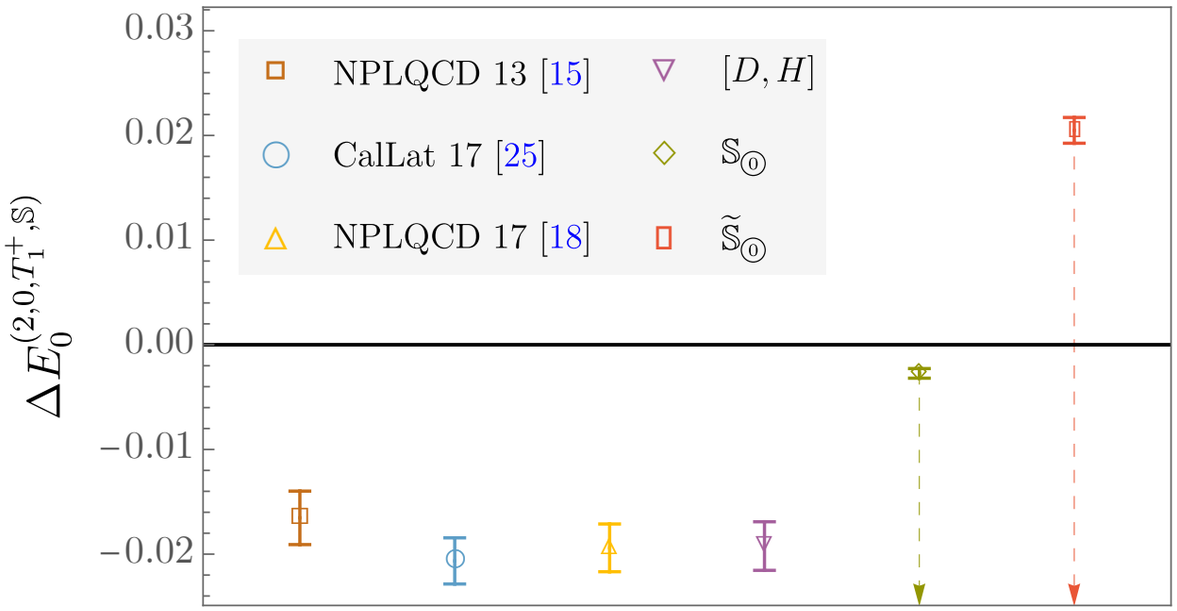

Ground-state energy **estimates** using different interpolating-operator sets show large discrepancies

Phase shifts obtained using asymmetric vs variational energy estimates suggest qualitatively different physics (bound vs unbound)

Amarasinghe, MW et al [NPLQCD], PRD 107 (2023)

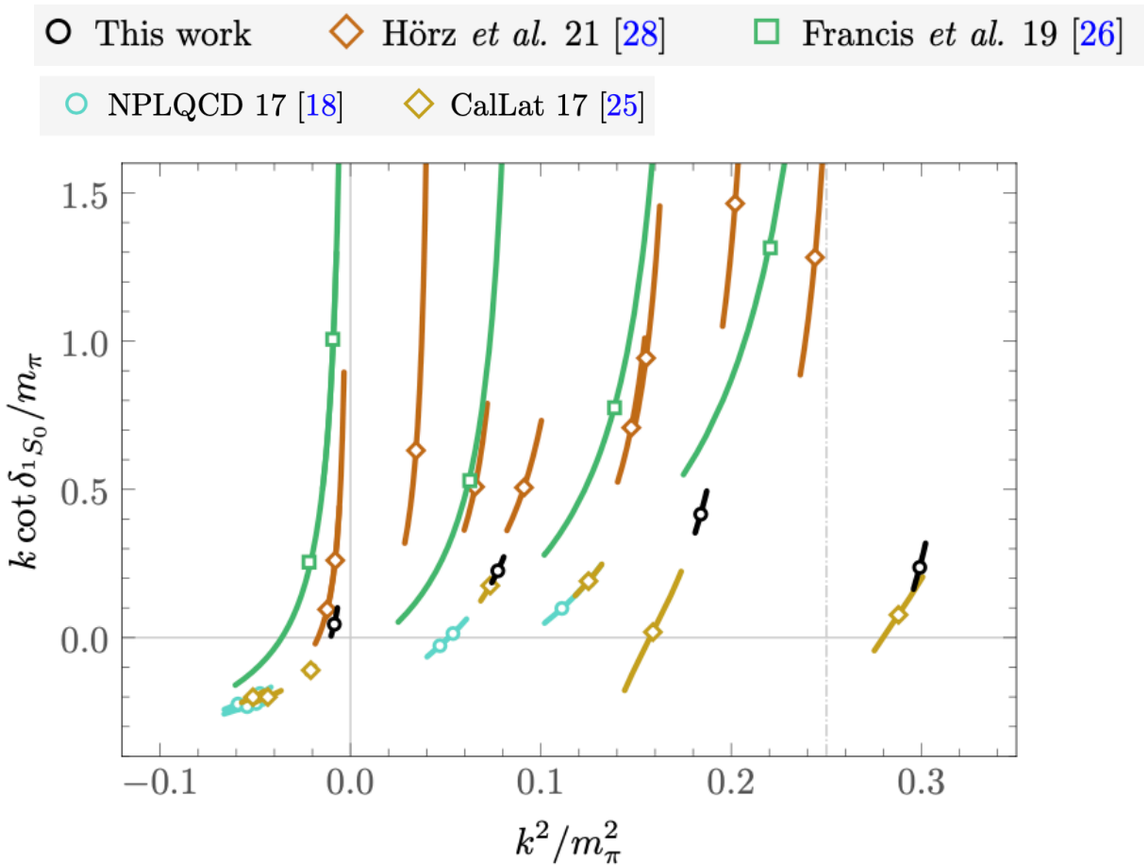

Results by different groups using similar interpolating operators show good consistency

Can we get more robust constraints than one-sided variational bounds?

Yes

(Block) Lanczos for Lattice QCD

MW, arXiv:2406.20009

Hackett, MW, arXiv:2407.21777

Hackett, MW, arXiv:2412.04444

Cornelius Lanczos

Daniel Hackett

Transfer-matrix eigenvalues

Lattice theories do not have continuous time translation symmetry defining Hamiltonian

$$\mathcal{O}(t) = e^{-Ht}\mathcal{O}e^{Ht}$$

Discrete time translation symmetry enables definition of transfer matrix T

$$\mathcal{O}(ka) = T^k\mathcal{O}(T^{-1})^k$$

Energy spectrum = - ln (spectrum of eigenvalues of T)

$$T\left|n\right\rangle = \left|n\right\rangle\lambda_n \qquad E_n = -\ln\lambda_n$$

Correlation functions are matrix elements of powers of T

$$C(t) \equiv \left\langle\psi(t)\psi^\dagger(0)\right\rangle = \left\langle\psi\right| T^{t/a} \left|\psi\right\rangle + \ldots$$

The power-iteration algorithm

Start with an arbitrary normalized initial state: $|b_1\rangle = |\psi\rangle/|\psi|$

Iteration step: $|p_{k+1}\rangle = T|b_k\rangle$ $|b_{k+1}\rangle = |p_{k+1}\rangle/|p_{k+1}|$

Convergence: $|b_k\rangle \propto T^{k-1}|\psi\rangle = e^{-(k-1)aE_0}|\psi\rangle Z_0 + O\left(e^{-k\delta}\right)$

The power-iteration algorithm

Start with an arbitrary normalized initial state: $\big|b_1\big\rangle = \big|\psi\big\rangle / |\psi|$

Iteration step: $\big|p_{k+1}\big\rangle = T\big|b_k\big\rangle$ $\quad \big|b_{k+1}\big\rangle = \big|p_{k+1}\big\rangle / |p_{k+1}|$

Convergence: $\big|b_k\big\rangle \propto T^{k-1}\big|\psi\big\rangle = e^{-(k-1)aE_0}\big|\psi\big\rangle Z_0 + O\left(e^{-k\delta}\right)$

Energies from power-iteration eigenvalues:

$$-\ln\big\langle b_k|T|b_k\big\rangle = -\ln\left[\frac{\big\langle\psi|T^{2k-1}|\psi\big\rangle}{\big\langle\psi|T^{2k-2}|\psi\big\rangle}\right] = aE_0 + O\left(e^{-k\delta}\right)$$

$$= -\ln\left[\frac{C((2k-1)a)}{C((2k-2)a)}\right] = aE^{\mathrm{eff}}(t/a = 2k-1)$$

Standard effective mass = “apply power-iteration algorithm to the transfer matrix”

Lanczos = Krylov + Rayleigh-Ritz

Start with an arbitrary normalized initial state: $\big|v_1\big\rangle = \big|\psi\big\rangle / |\psi| = \big|\psi\big\rangle / \sqrt{C(0)}$

Iteration step:

$$\big|v_{j+1}\big\rangle \beta_{j+1} = (T - \alpha_j)\big|v_j\big\rangle - \beta_j \big|v_{j-1}\big\rangle$$

Where $\alpha_j = \big\langle v_j | T | v_j \big\rangle \quad \beta_j = \big\langle v_{j-1} | T | v_j \big\rangle$

Lanczos (1950)

See Parlett, "The Symmetric Eigenvalue Problem" (1980)

Novel features not present in power iteration

- Lanczos vectors form orthonormal basis for Krylov space

$$\mathcal{K}^{(m)} = \mathrm{span}\{\big|v_1\big\rangle, \big|v_2\big\rangle, \ldots, \big|v_m\big\rangle\}$$

$$\big\langle v_i | v_j \big\rangle = \delta_{ij}$$

- Krylov-space approximation to T directly computable

$$T_{ij}^{(m)} = \big\langle v_i | T | v_j \big\rangle = \delta_{ij}\alpha_j + \delta_{i(j-1)}\beta_j + \delta_{i(j+1)}\beta_{j+1}$$

Krylov space ~ span of data ~ computationally accessible part of Hilbert space

Optimal estimators given fixed data

Krylov-space approximation to T directly computed in Lanczos algorithm

- It's eigenvalues provide "best" Krylov-space approximations to T eigenvalues

$$T_{ij}^{(m)} = \langle v_i | T | v_j \rangle = \begin{pmatrix} \alpha_1 & \beta_2 & & & & 0 \\ \beta_2 & \alpha_2 & \beta_3 & & & \\ & \beta_3 & \alpha_3 & \ddots & & \\ & & \ddots & \ddots & \beta_{m-1} & \\ & & & \beta_{m-1} & \alpha_{m-1} & \beta_m \\ 0 & & & & \beta_m & \alpha_m \end{pmatrix}_{ij}$$

Diagonalize the Krylov-space transfer matrix:

$$T_{ij}^{(m)} = \sum_k \omega_{ik}^{(m)} \lambda_k^{(m)} (\omega^{-1})_{kj}^{(m)}$$

"Ritz values" = optimal Krylov-space approximation to T eigenvalues

"Ritz vectors" = corresponding approximate eigenstates

$$|y_k^{(m)}\rangle = \sum_j |v_j\rangle \omega_{jk}^{(m)}$$

$$\lambda_k^{(m)} = \langle y_k^{(m)} | T | y_k^{(m)} \rangle$$

Lanczos without Lanczos vectors

Problem: In LQCD, we don't have direct access to infinite-dimensional Hilbert space vectors

Lanczos without Lanczos vectors

Problem: In LQCD, we don't have direct access to infinite-dimensional Hilbert space vectors

Solution: Compute the matrix elements $T_{ij}^{(m)}$ directly from correlation functions via recursion relations:

MW, arXiv:2406.20009

$$\alpha_1 = \langle v_1 | T | v_1 \rangle = \frac{C(1a)}{C(0)} \qquad \beta_1 = 0$$

Recursive Lanczos iteration:

$$A_j^k = \langle v_j | T^k | v_j \rangle \quad B_j^k = \langle v_{j-1} | T^k | v_j \rangle$$

$$\beta_{j+1} = \sqrt{A_j^2 - \alpha_j^2 - \beta_j^2}$$

$$B_{j+1}^k = \frac{1}{\beta_{j+1}} [A_j^{k+1} - \alpha_j A_j^k - \beta_j B_j^k]$$

• • •

Ritz values reproduce spectrum of 12-state toy model exactly after 12 steps:

$$C(t) = \sum_{n=1}^{12} \frac{1}{2(0.1n)} e^{-0.1nt}$$

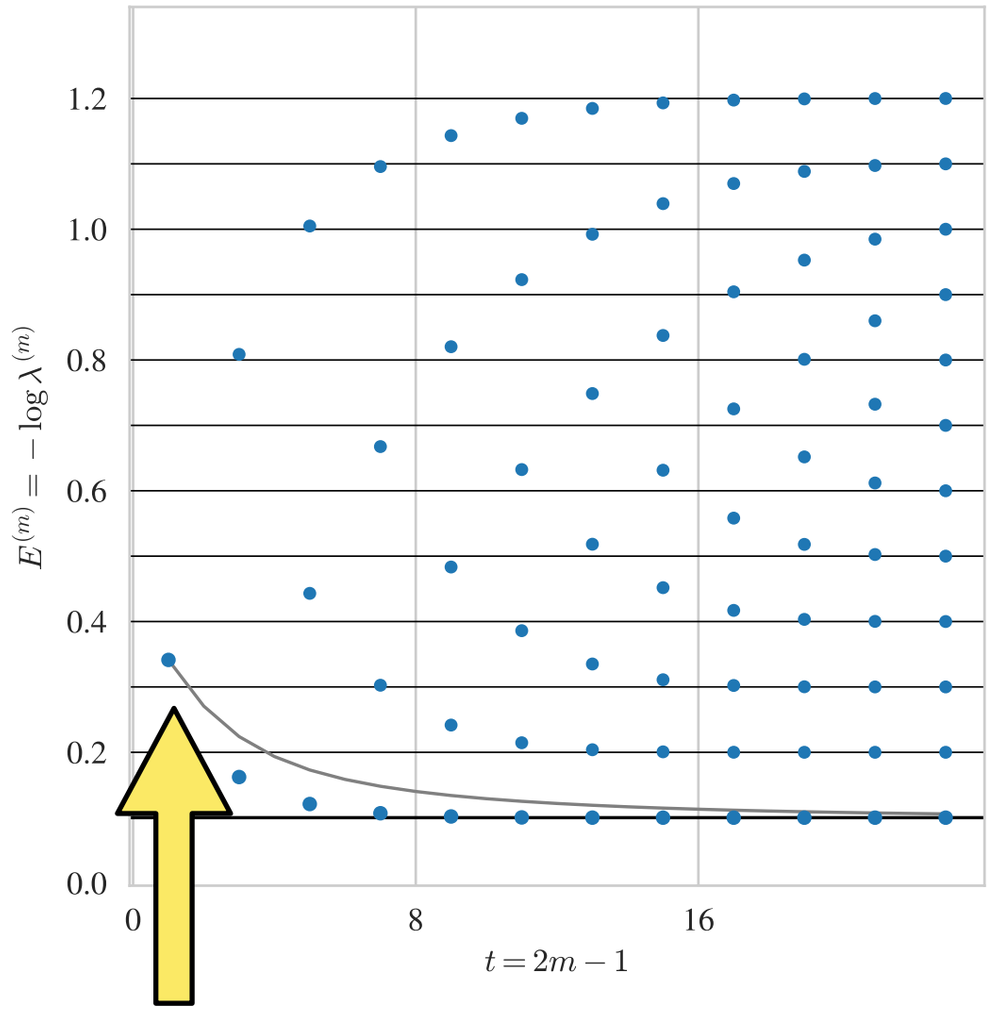

Lanczos equals power iteration after $m = 1$ step, converges faster for $m > 1$

Residual bounds

- Lanczos approximation error after finite number of iterations directly computable:

$$\min_{\lambda \in \{\lambda_n\}} |\lambda_0^{(m)} - \lambda| \leq |\beta_{m+1} \omega_{m0}^{(m)}|$$

Eigenvectors of $T^{(m)}$

Matrix element $T^{(m)}_{m(m+1)}$

See Parlett, The Symmetric Eigenvalue Problem (1980)

Rigorous quantification of excited-state effects!

Mock data tests demonstrate

- Lanczos converges exponentially faster than power iteration / effective mass
- Residual bound provides valid two-sided bound on errors from excited-state effects

Note: residual bound is on distance to closest eigenvalue, not e.g. "true ground state"

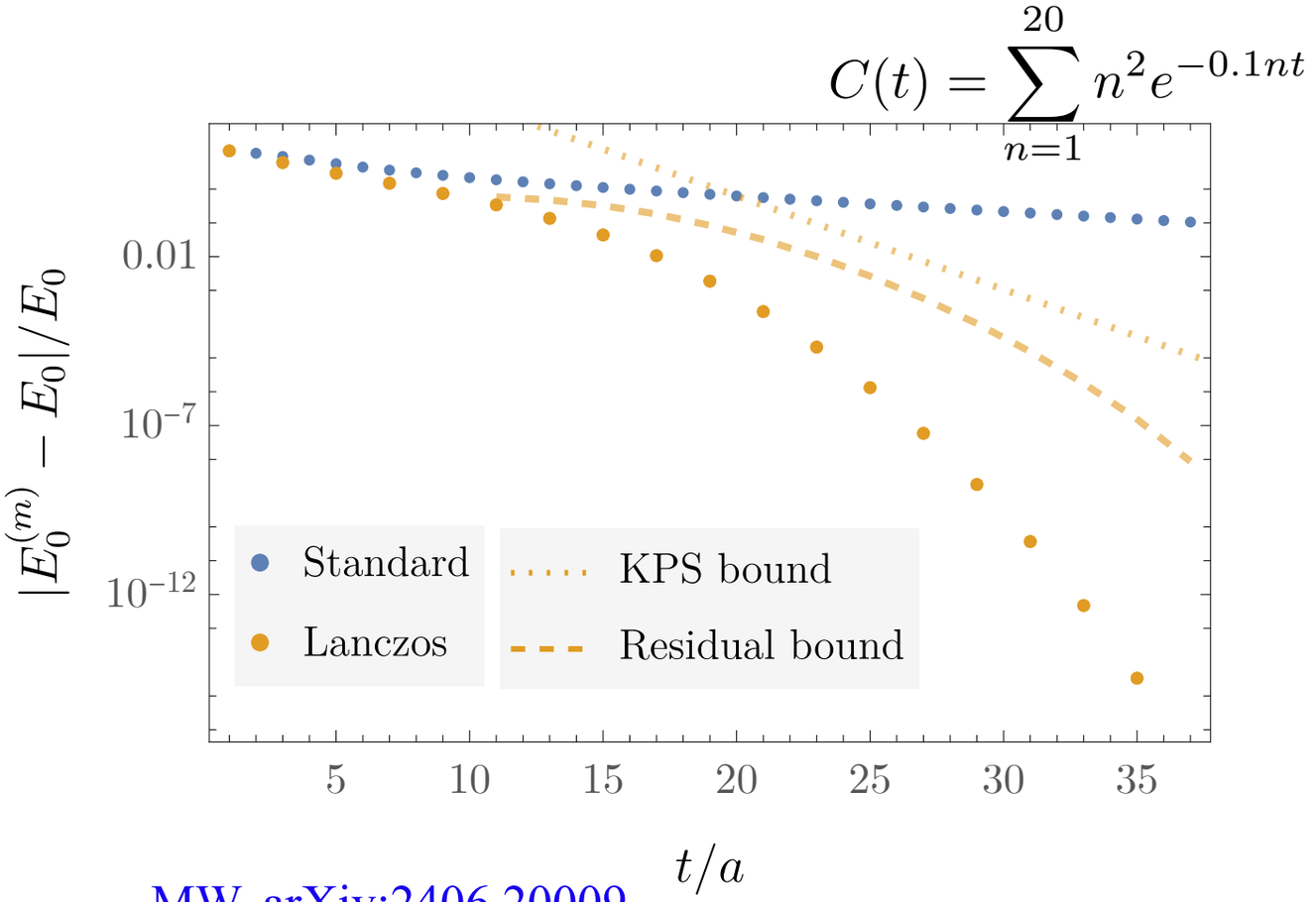

MW, arXiv:2406.20009

Spurious eigenvalues

Decades of research on how roundoff affects Lanczos has led to an understanding of the "Lanczos phenomenon"

- Roundoff leads to O(1) errors in some "spurious" Ritz values that do not converge
- Remaining "non-spurious" Ritz values still accurate, converge to eigenvalues

Statistical noise leads to unphysical Ritz values:

- Most Ritz values complex even though transfer matrix eigenvalues real + positive
- Taking real parts at face value would give ground-state energy violating QCD inequality $M_N > m_\pi$

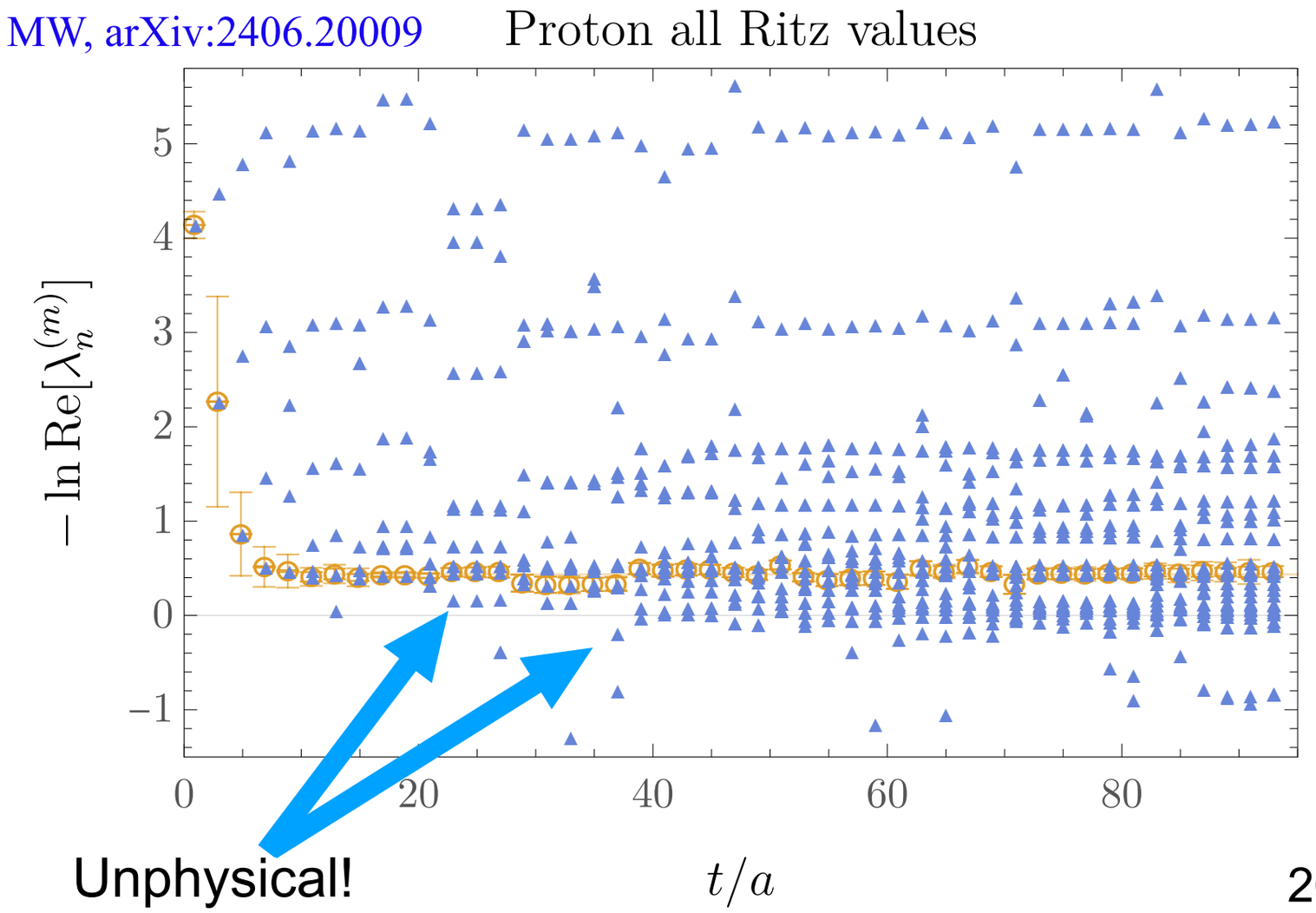

The physics of noise

Krylov space can be decomposed into sectors based off Ritz properties

$$T^{(m)} = \sum_{k\in\overline{\mathcal{S}}} \lambda_k^{(m)} \left|y_k^{(m)}\right\rangle\left\langle y_k^{(m)}\right| + \sum_{k\in\mathcal{S}} \lambda_k^{(m)} \left|y_k^{L(m)}\right\rangle\left\langle y_k^{R(m)}\right|$$

Non-spurious

Spurious

Further classification of spurious states possible:

- Non-spurious ⊂ Hermitian subspace ⊂ Real Ritz values

Unphysical states (e.g. with complex norms) needed to describe data that is non-convex in the presence of noise

States with non-zero initial-state overlap (“correct quantum numbers”) are unaffected by spurious state filtering, can be interpreted physically

Hackett, MW, arXiv:2412.04444

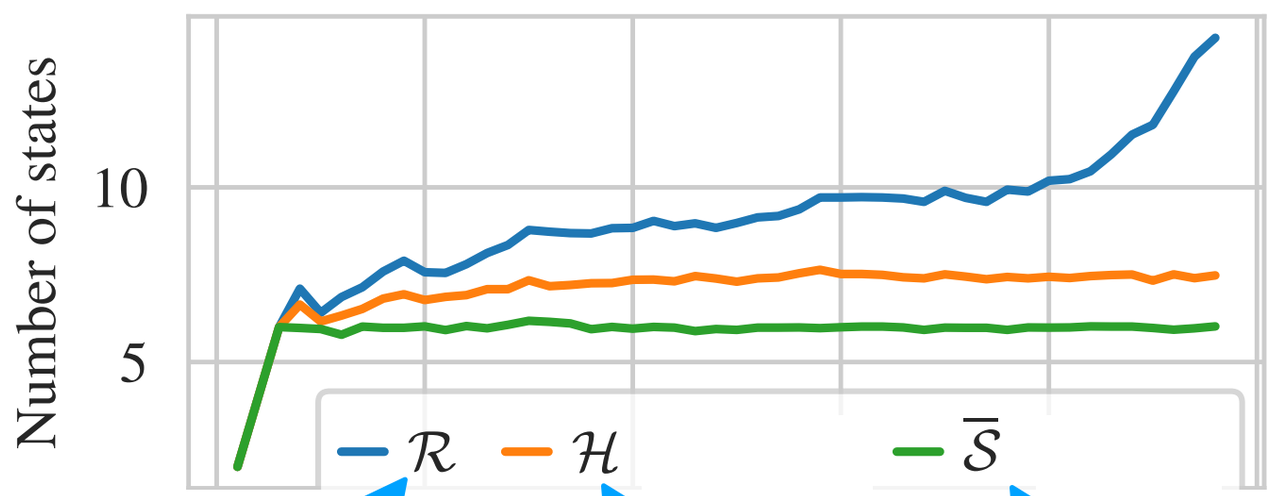

Real Ritz values

Hermitian subspace

Non-spurious subspace

The ZCW test

Roundoff (and noise) leads to errors in orthogonalization, artificially extend Krylov space in spurious directions Paige (1971) Parlett and Scott (1979)

- Motivates “Cullum-Willoughby test”: spurious directions should only depend on numerical artifacts and be independent of initial vector

  Cullum and Willoughby, Journal of Computational Physics 44, 329 (1981)

The ZCW test

Roundoff (and noise) leads to errors in orthogonalization, artificially extend Krylov space in spurious directions Paige (1971) Parlett and Scott (1979)

- Motivates "Cullum-Willoughby test": spurious directions should only depend on numerical artifacts and be independent of initial vector

  Cullum and Willoughby, Journal of Computational Physics 44, 329 (1981)

Physically: independence of initial vector ~ zero overlap with source ~ wrong quantum numbers

ZCW test for spuriously small overlaps

Hackett, MW, arXiv:2412.04444

$$\Delta_k^{\mathrm{ZCW}(m)} = \left| \frac{Z_k^{R(m)*} Z_k^{L(m)}}{C(0)} \right| < \varepsilon^{\mathrm{ZCW}}$$

Eigenvalue-eigenvector identity* can be used to prove equivalence of CW and ZCW tests for small $\varepsilon^{\mathrm{ZCW}} \sim \varepsilon^{\mathrm{CW}}$

Size of overlaps on last iteration where all Ritz values obey all physical constraints sets natural scale for $\varepsilon^{\mathrm{ZCW}}$

* See Denton, Parke, Tao, and Zhang, Bull. Am. Math Soc. 59, 31 (2022)

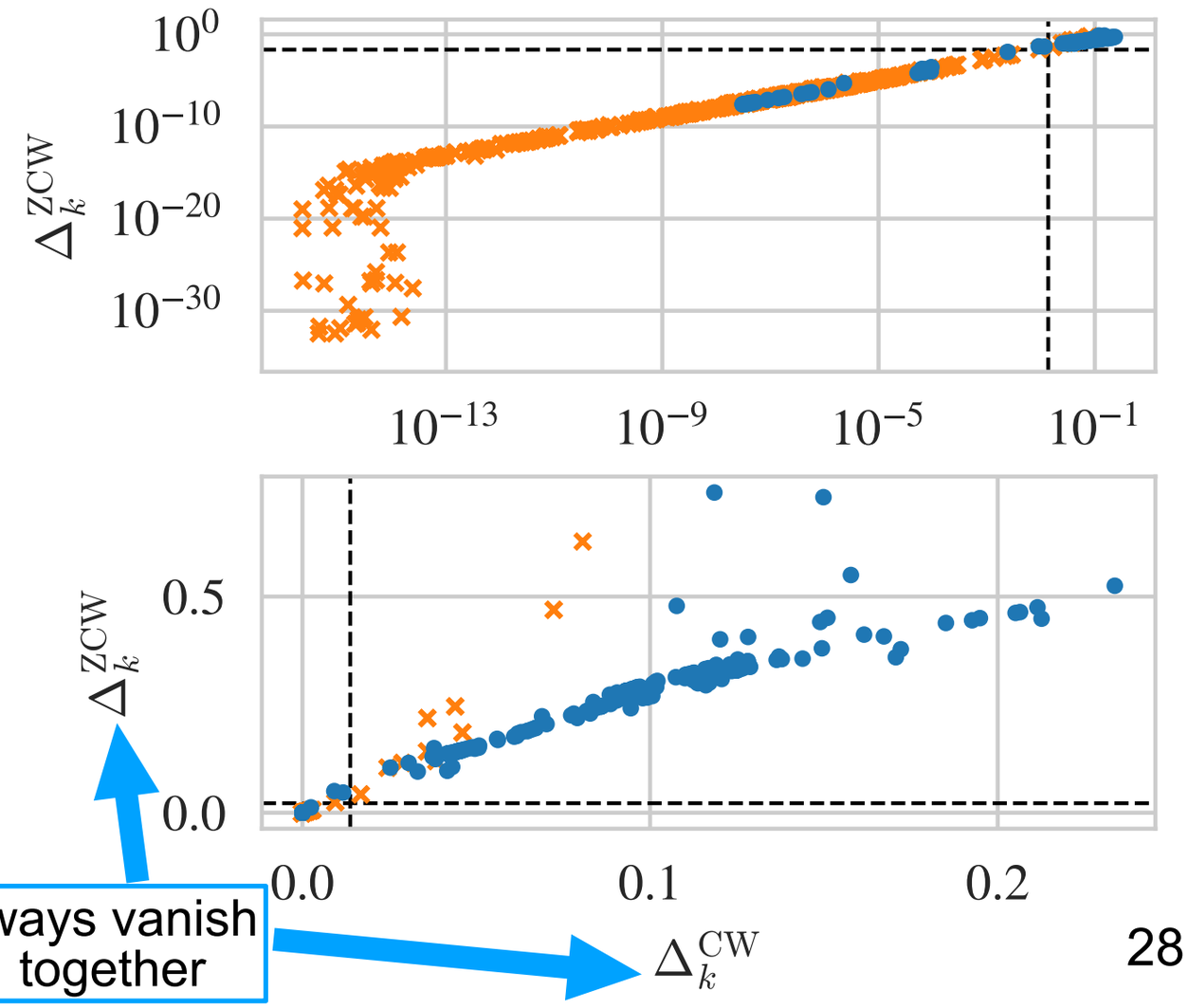

Non-spurious energies are accurate

All obviously unphysical proton eigenvalues removed by “spurious-state filtering” using the CW or ZCW test

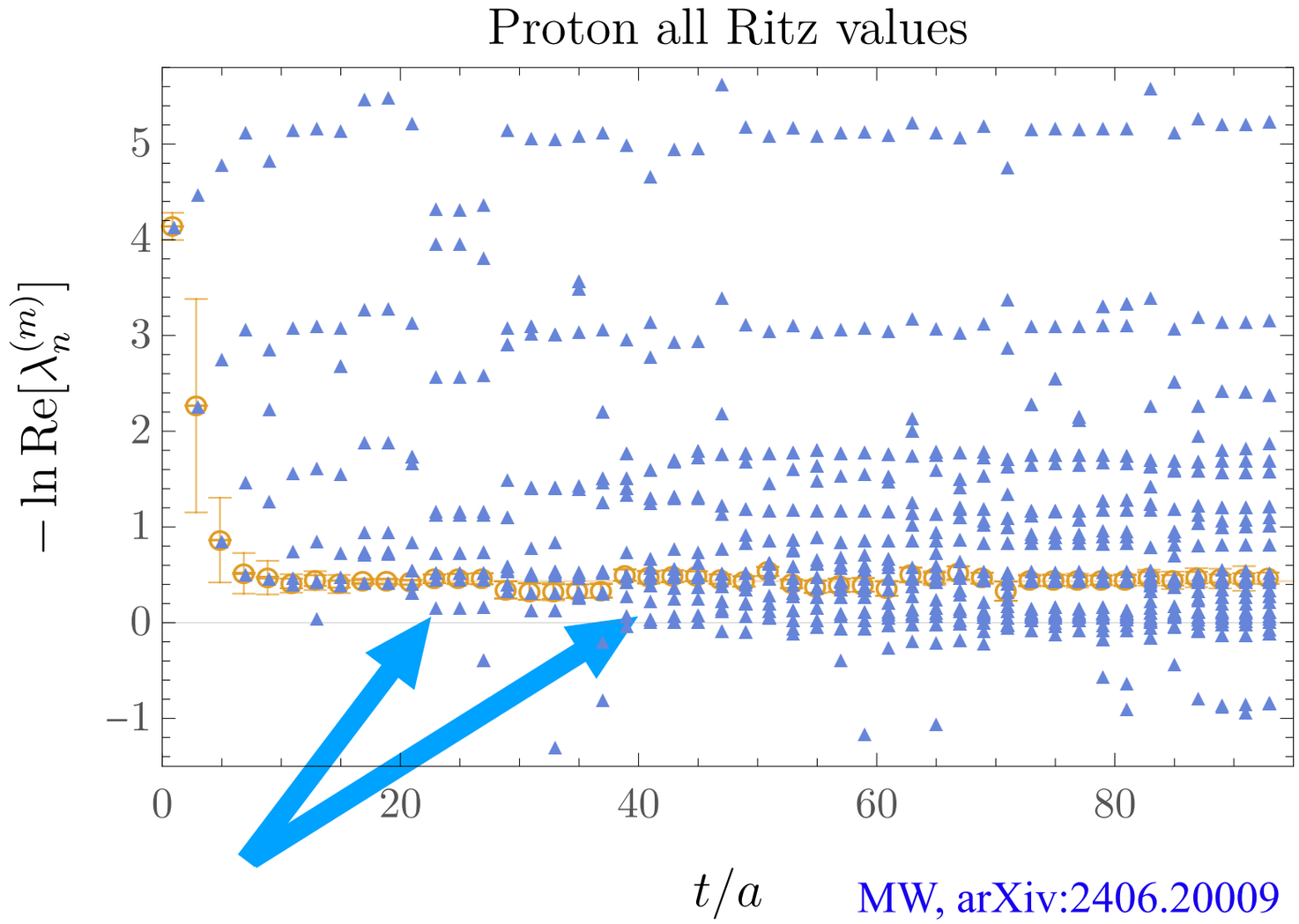

MW, arXiv:2406.20009

Non-spurious energies are accurate

All obviously unphysical proton eigenvalues removed by “spurious-state filtering” using the CW or ZCW test

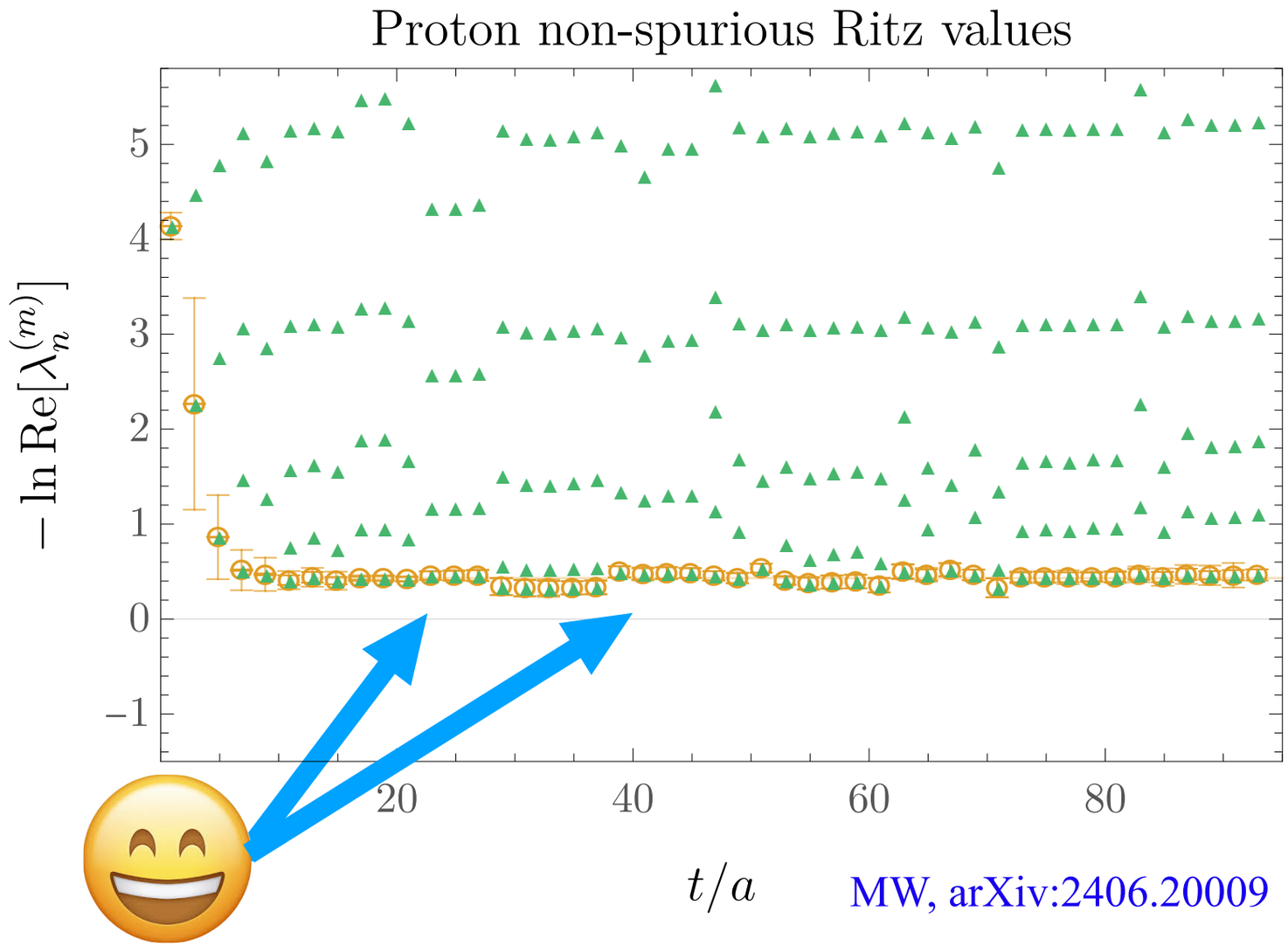

MW, arXiv:2406.20009

Non-spurious energies are accurate

All obviously unphysical proton eigenvalues removed by “spurious-state filtering” using the CW or ZCW test

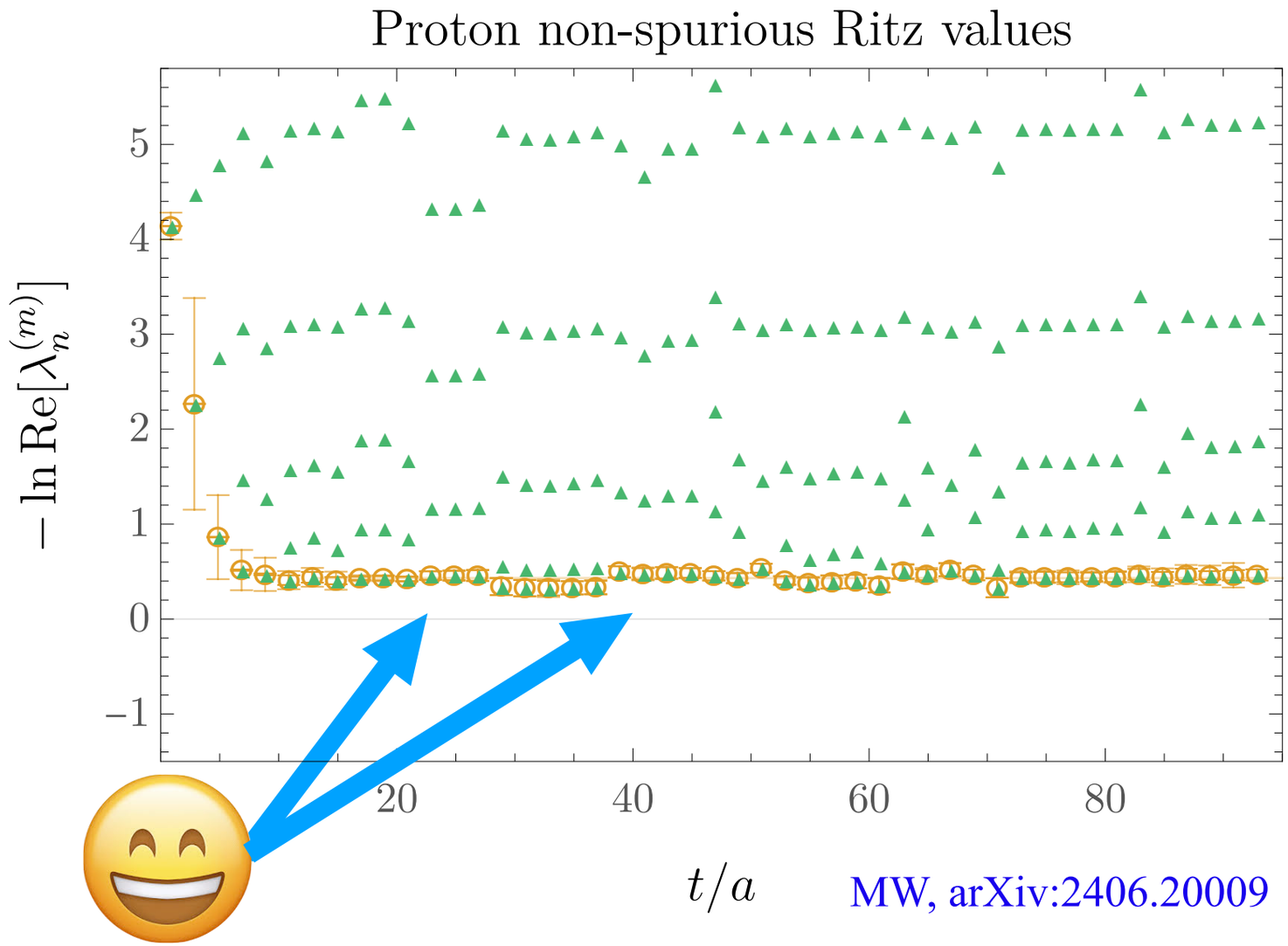

MW, arXiv:2406.20009

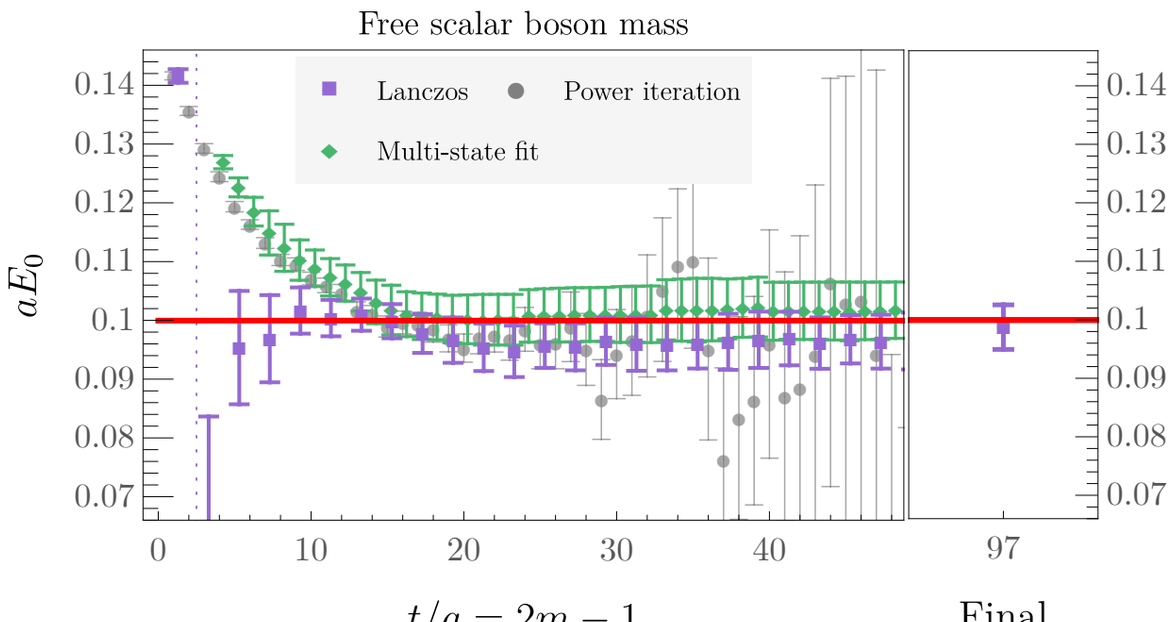

Defining $\lambda_0^{(m)}$ as the largest “non-spurious” Ritz value leads to accurate ground-state energy determinations in solvable models (e.g. free scalar field)

No fitting needed

Spurious state filtering isn't perfect — outlier robust estimators can be both more precise + accurate

- Use bootstrap median as estimator, compute uncertainties with nested bootstrap
- Large correlations appear for large m with bootstrap median, washed out in sample mean
- Energy distributions closer to Gaussian for bootstrap median

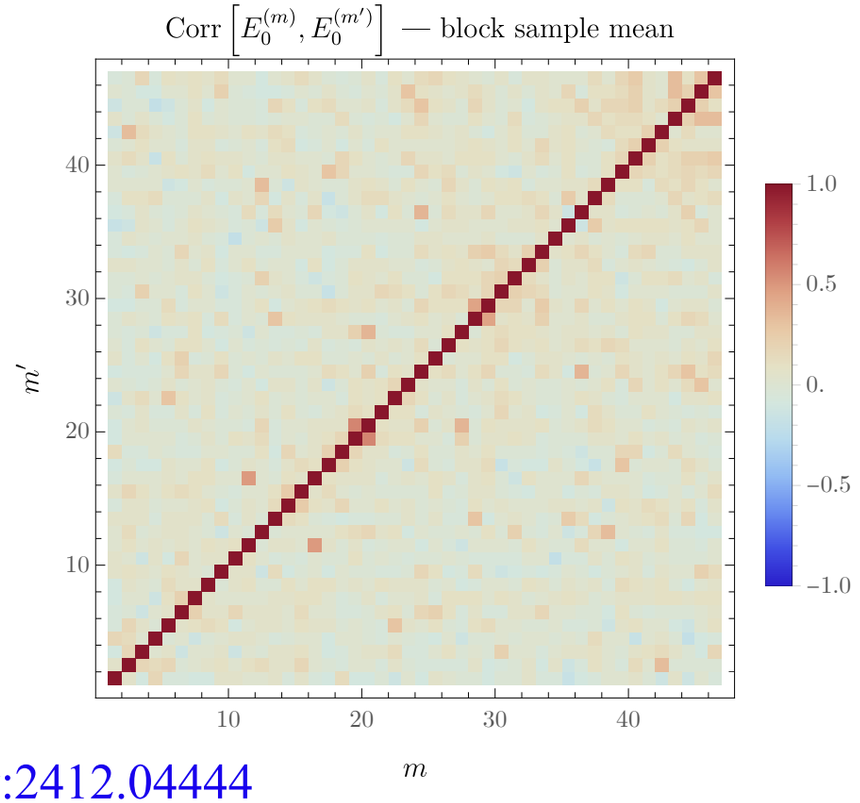

Hackett, MW, arXiv:2412.04444

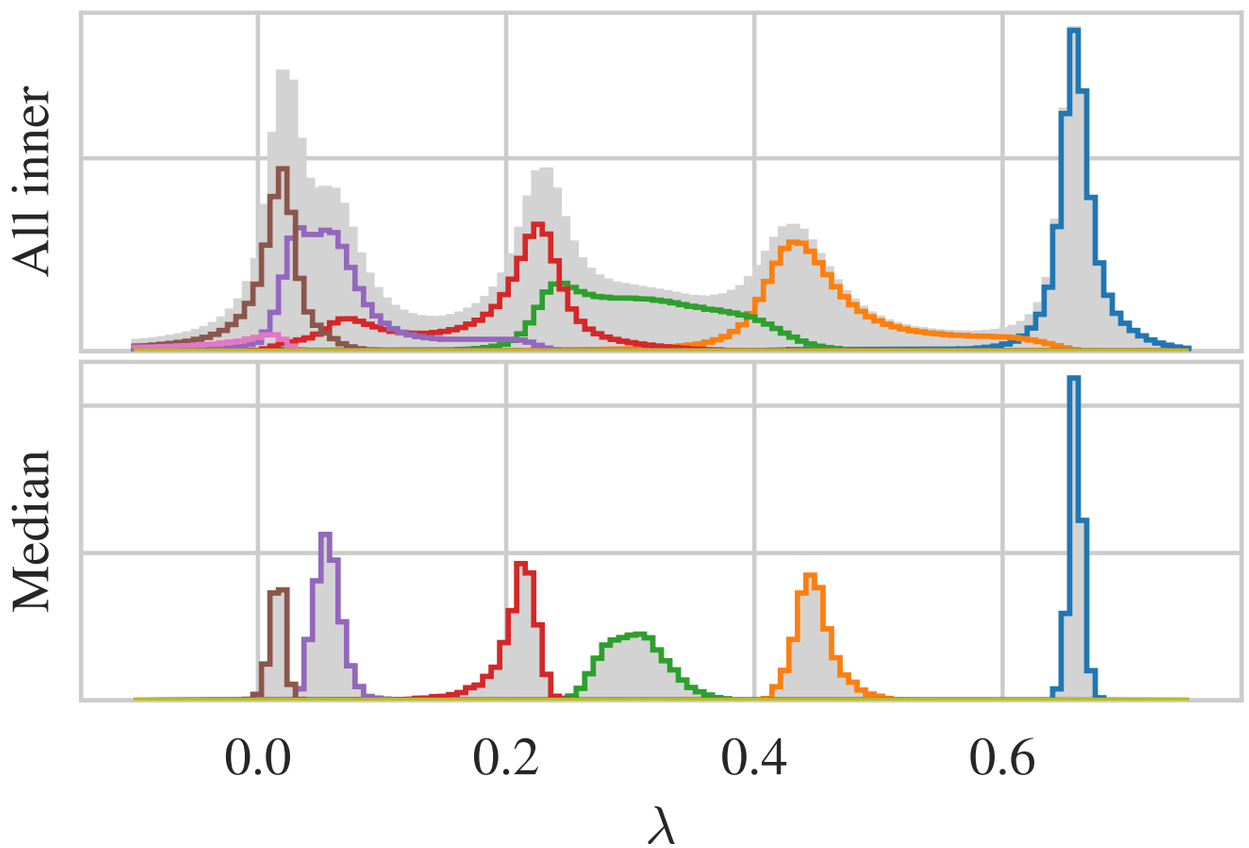

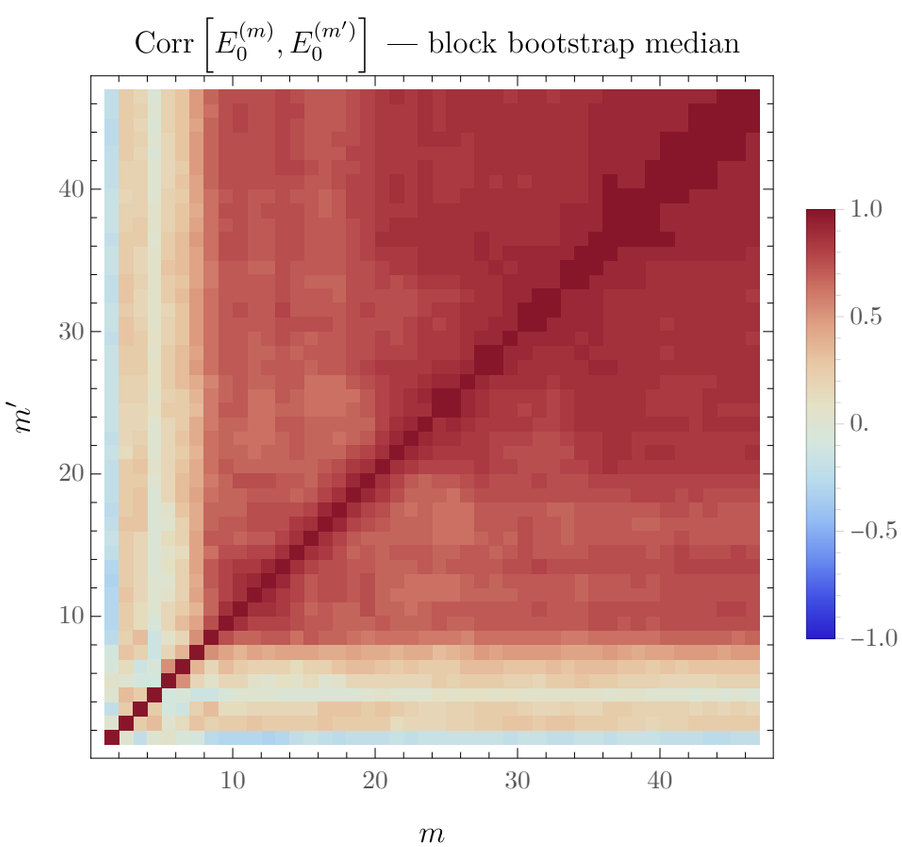

Asymptotically constant SNR

Bootstrap median estimators provide comparable uncertainties to multi-state fits with $t_{\max} = 2m - 1$

Given large correlations at large m, sufficient to define energy estimator from final iteration

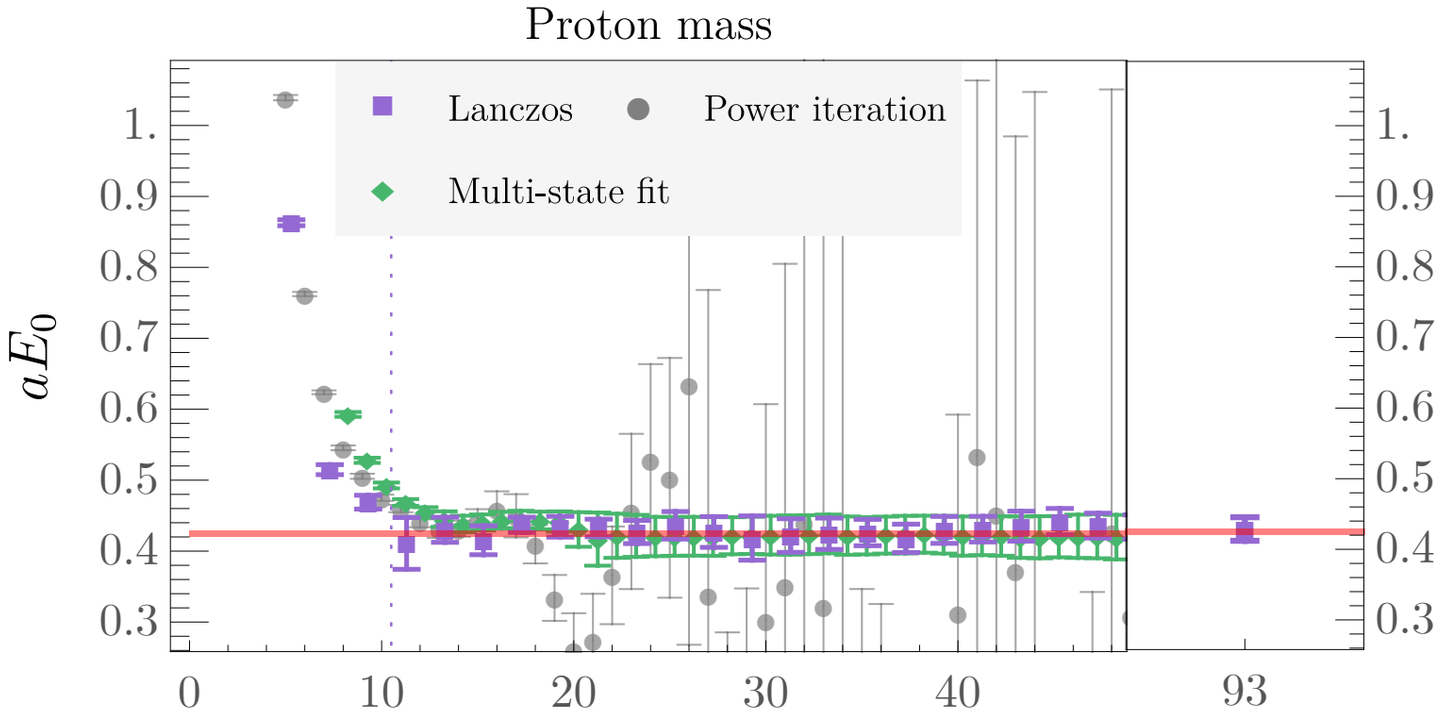

Variance saturates to constant value for large m, comparable to saturation of multi-state fit results

- Contrasts with power-iteration / effective mass, which exponentially approaches 0 SNR

Systematic bias due to O(1) phase fluctuations

$t/a = 2m - 1$ Final

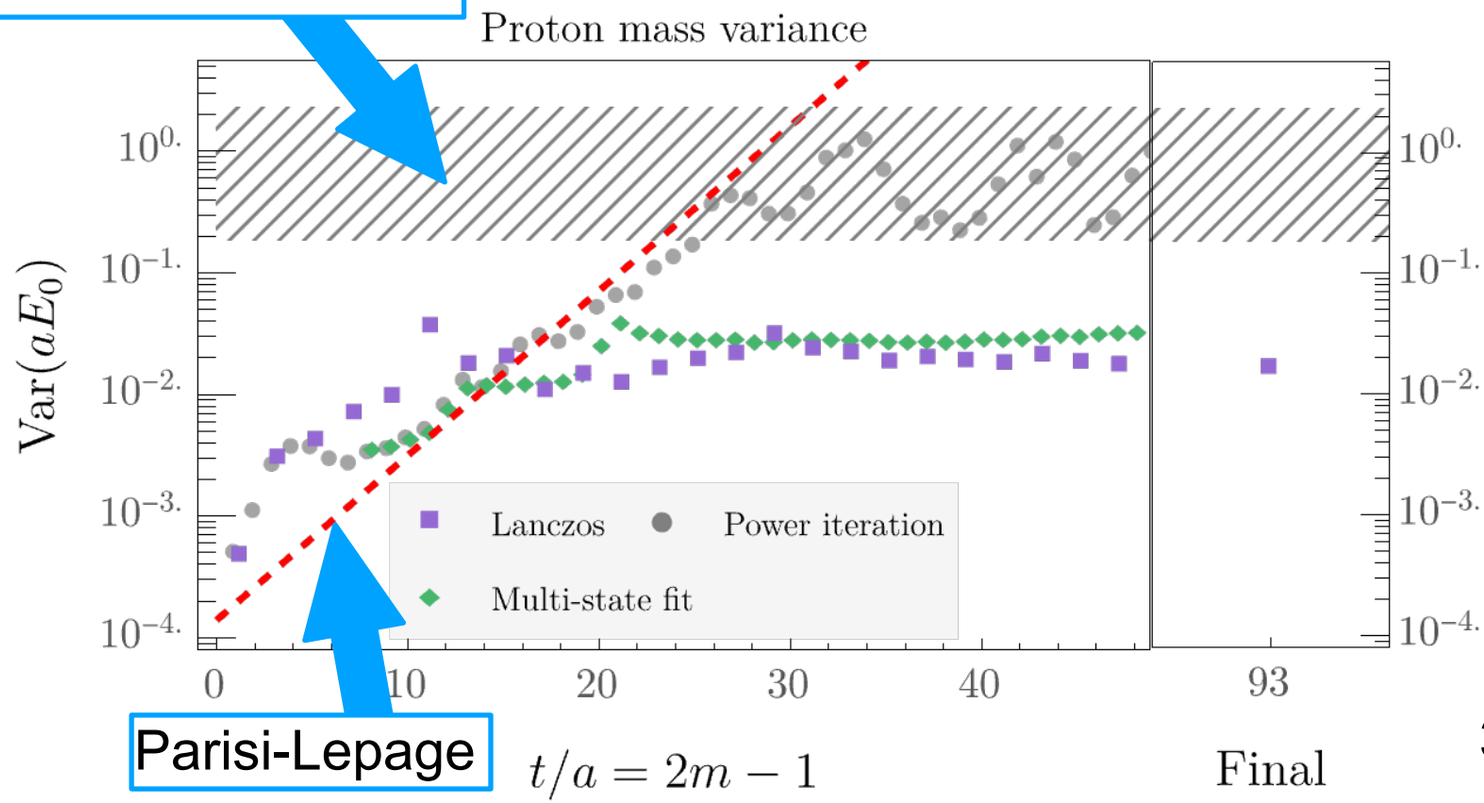

Parisi-Lepage

$t/a = 2m - 1$ Final

Block Lanczos and GEVP: Es

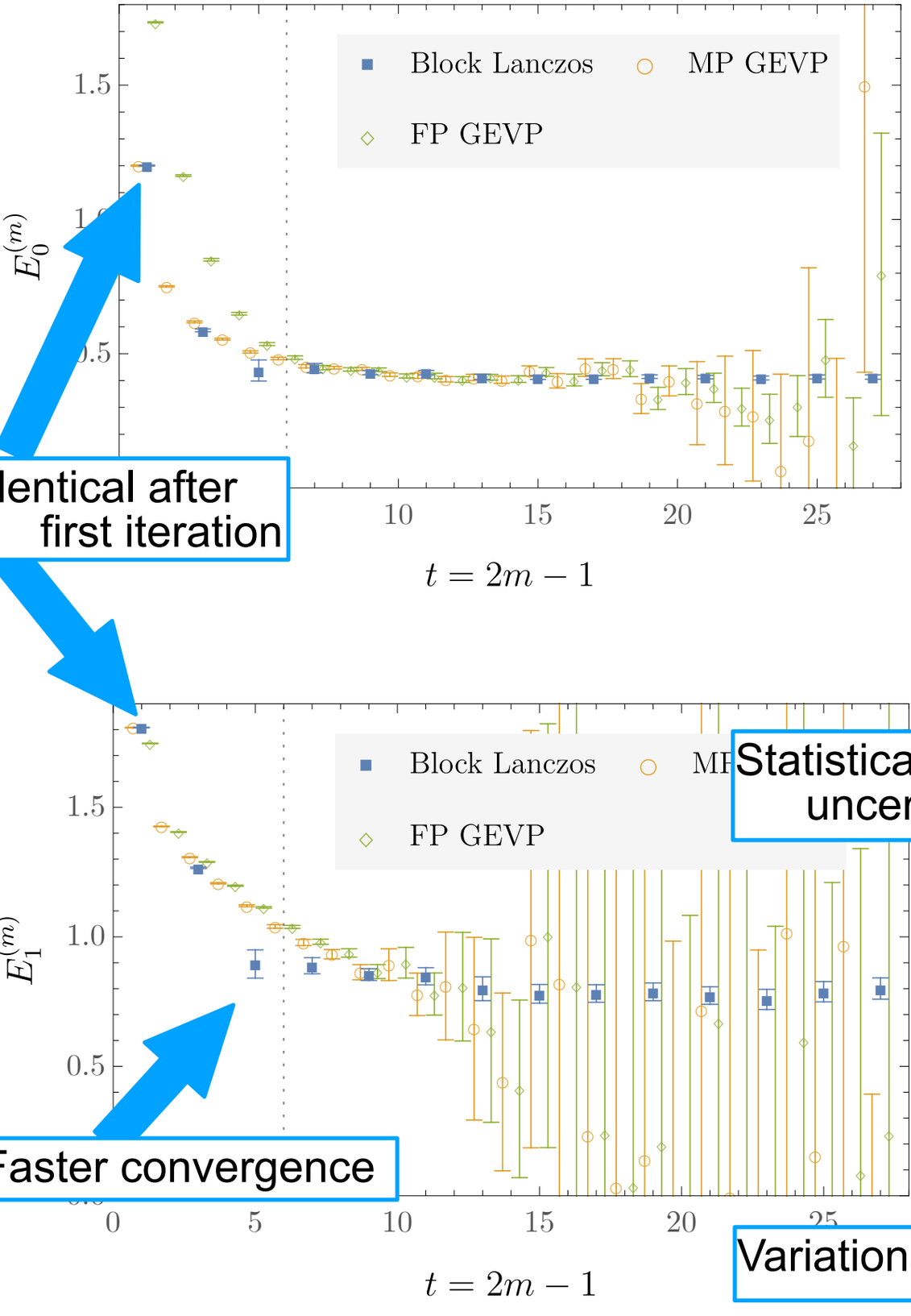

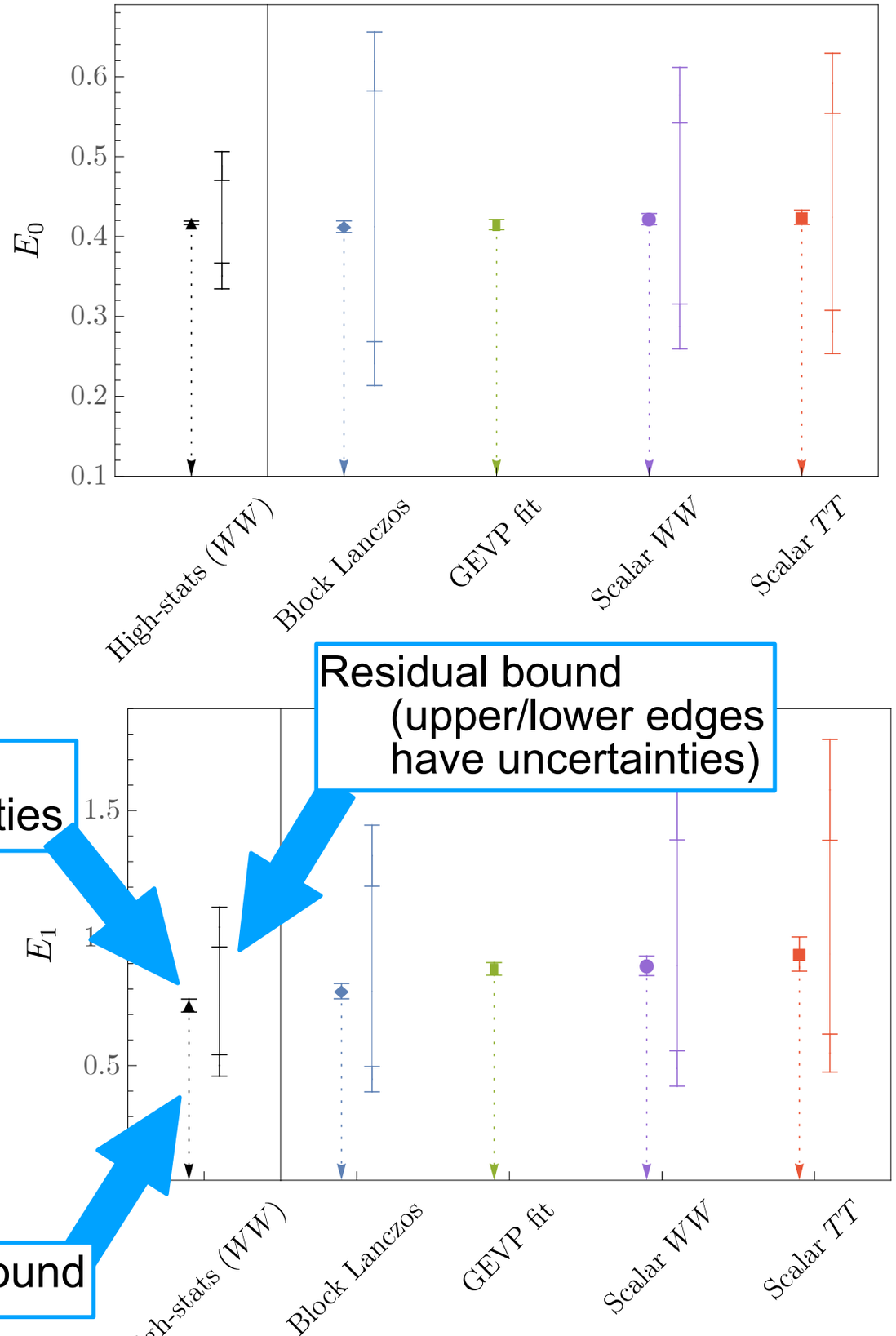

Block Lanczos and GEVP: Zs

Block Lanczos provides unambiguous signals for ground- and excited-state overlap factors

- Consistent with GEVP when the latter achieves reliable plateaus

- More robust signals for noisy excited-state observables

Deceptive pseudo-plateau?

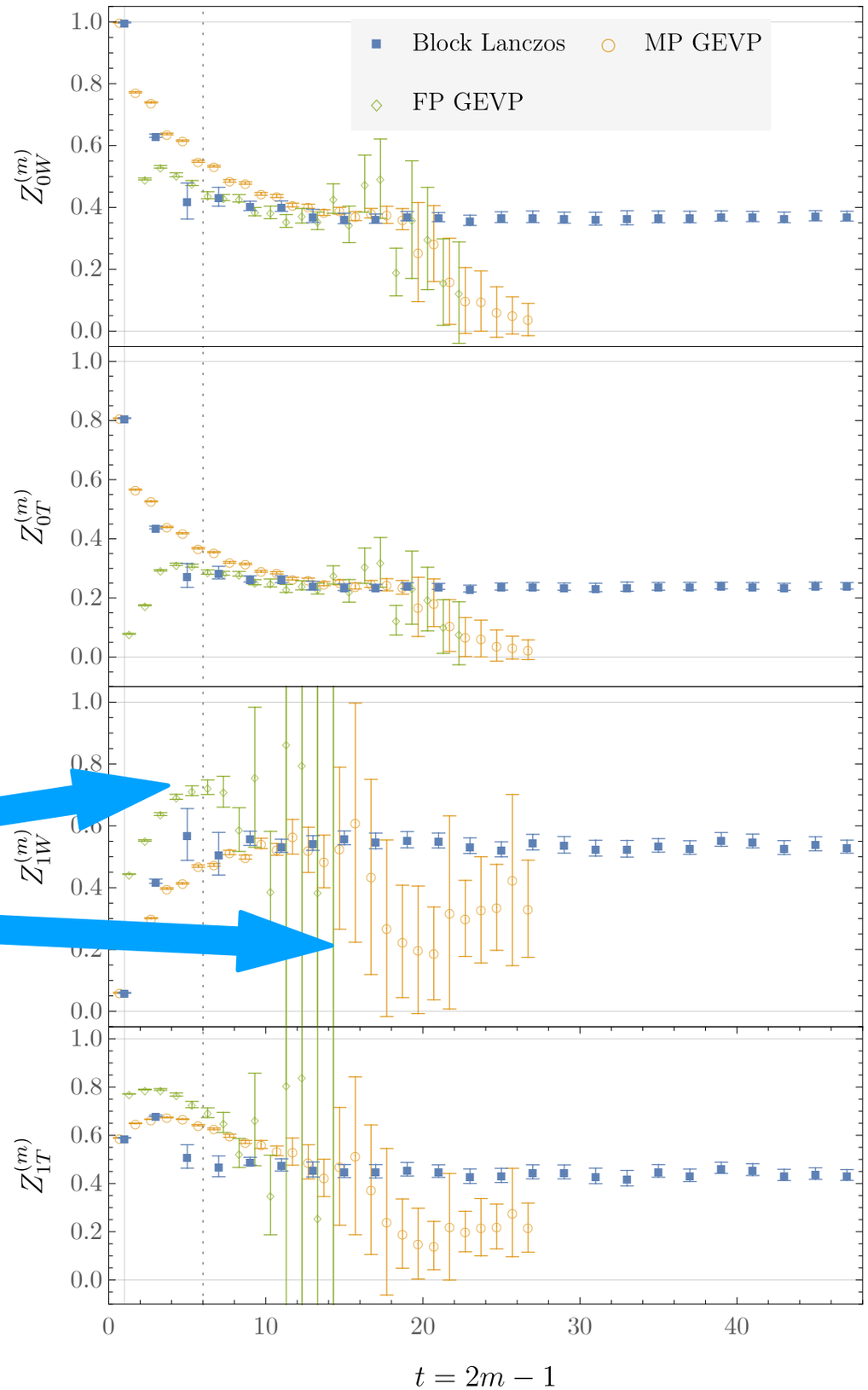

Block Lanczos and GEVP: Zs

Block Lanczos provides unambiguous signals for ground- and excited-state overlap factors

- Consistent with GEVP when the latter achieves reliable plateaus

- More robust signals for noisy excited-state observables

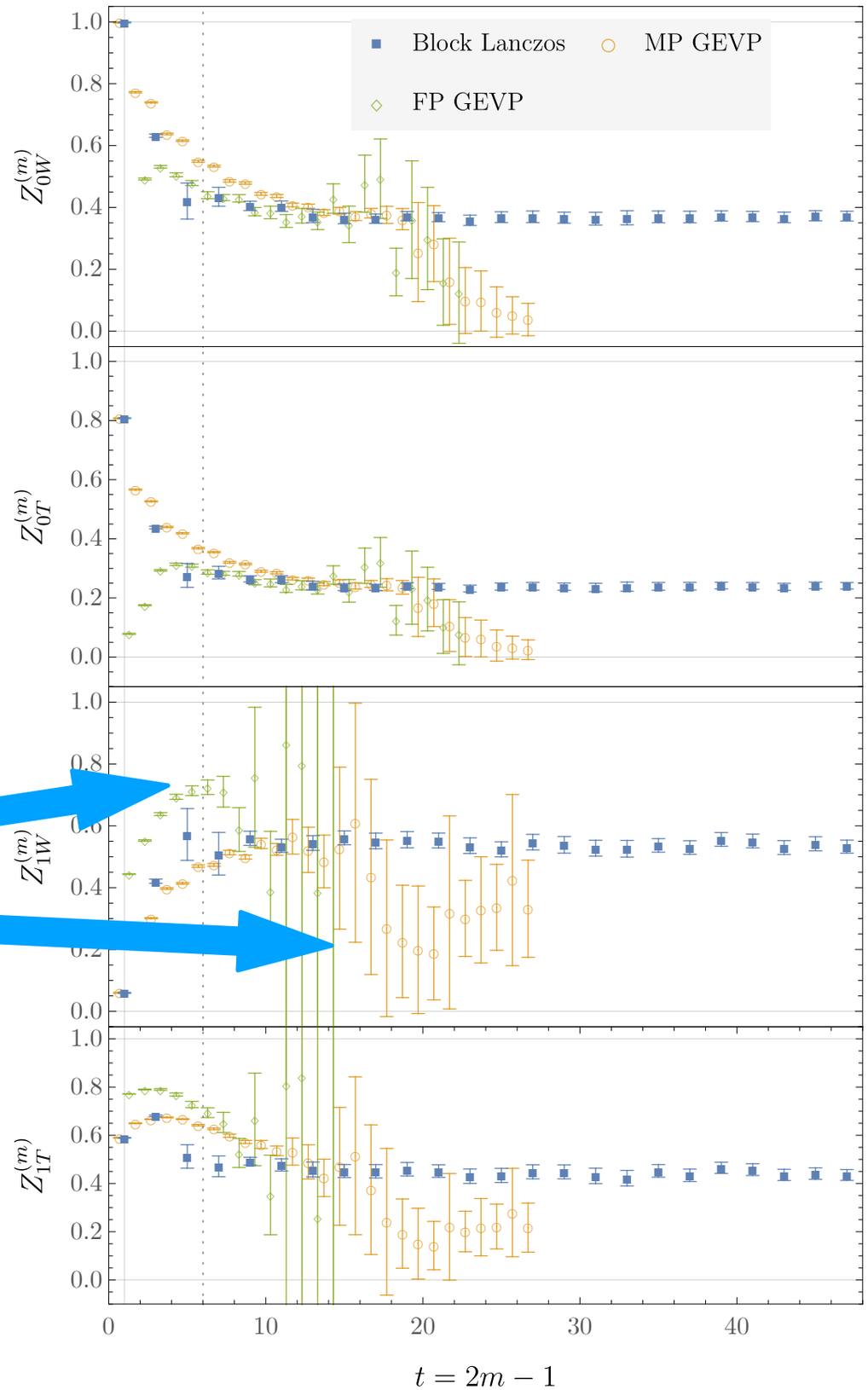

Deceptive pseudo-plateau?

Block Lanczos can be applied to nn correlator matrices to extract

$$\mathcal{Z}_{\mathsf{n}H_i^{nn}} = \langle 0|H_i^{nn}|nn,\mathsf{n}\rangle = \sum_J \langle 0|Q_J|nn,\mathsf{n}\rangle\, C_{Ji}$$

Outlook

Reliably interpreting experimental searches for intranuclear $n\bar{n}$ requires better understanding of nuclear effects on $\Delta B = 2$ matrix elements

nn decay — simplest starting point ?

$$\left\langle Q_I(t) nn^\dagger(0) \right\rangle \sim \sum_J \langle 0|Q_J|nn\rangle \, Z_{JI} + \ldots$$

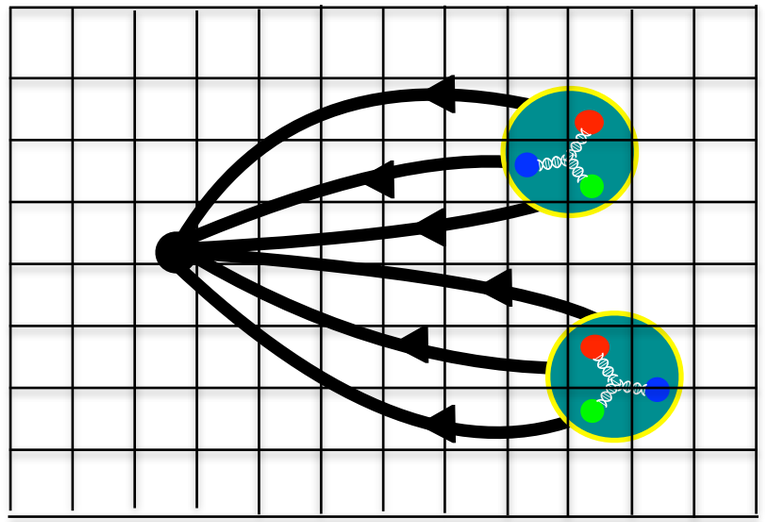

Exploratory results show significant energy dependence, hints that intranuclear $n\bar{n}$ depends nontrivially on neutron energy distribution

Lanczos methods provide a path to rigorously quantifying excited-state effects and providing robust QCD predictions for nn decay

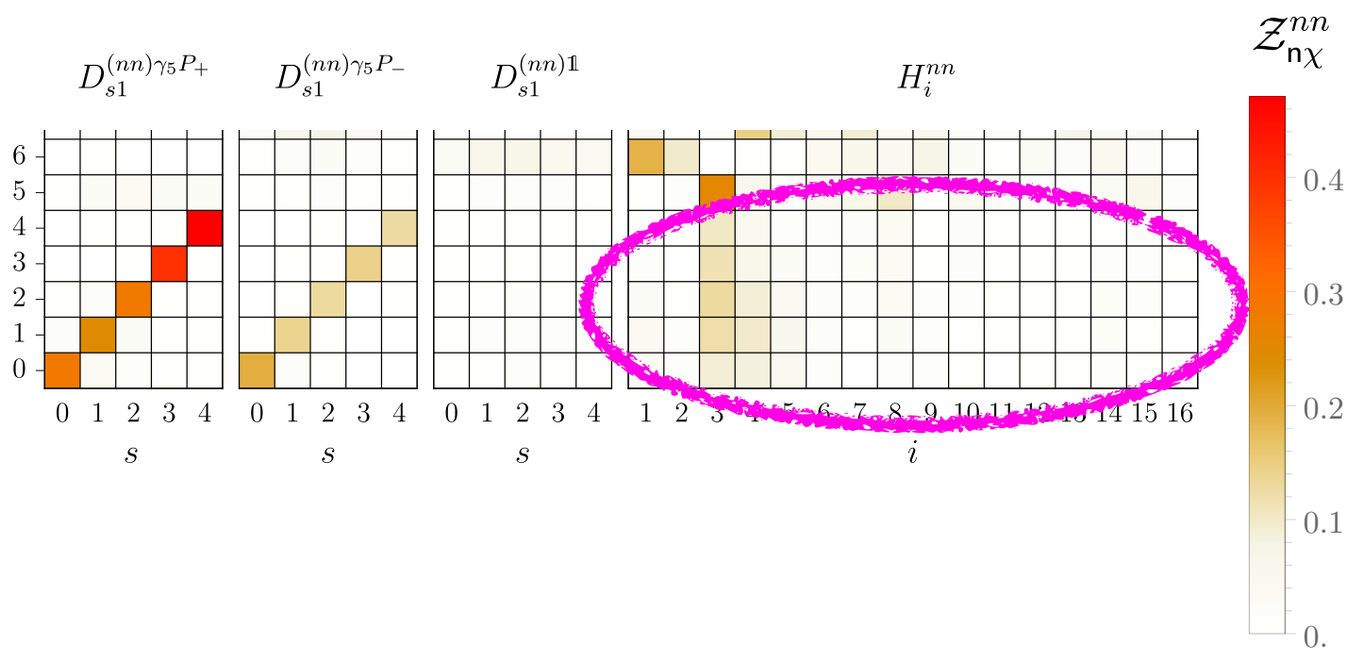

Backup

Excited-states or overlap problem?

Apparent plateau of hexaquark-dibaryon correlation function can be reproduced by a linear combination of ground- and excited-state GEVP energy levels

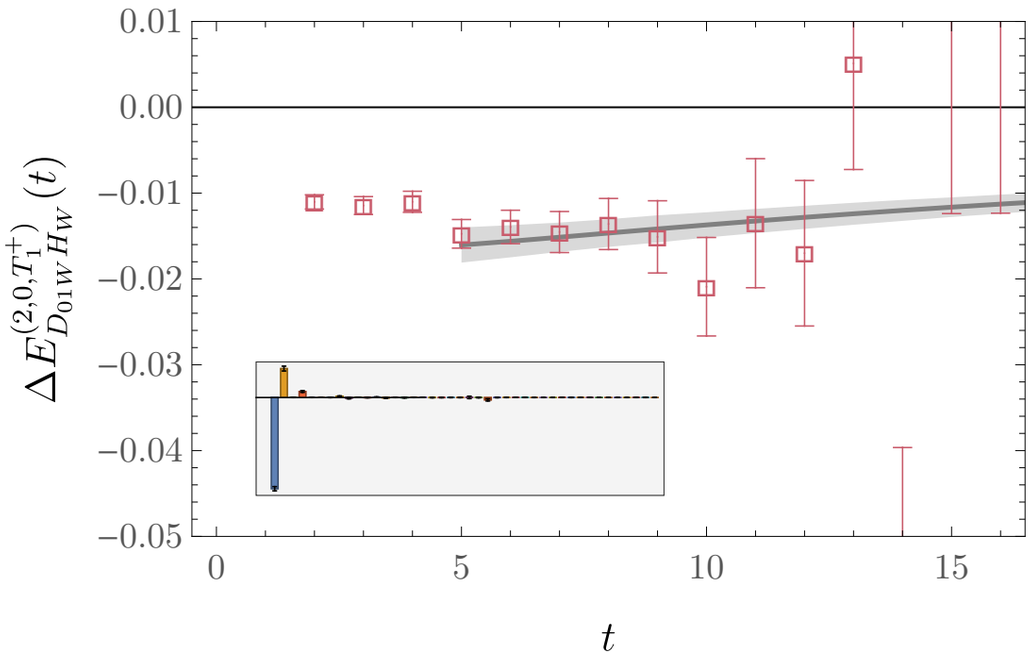

GEVP predicts slow approach to -0.0025(5) for much larger

$$t \gtrsim 1/(E_1 - E_0) \approx 41$$

Toy model: 2 operators, 3 states

$$Z_{\mathsf{n}}^{(A)} = (\epsilon, \sqrt{1-\epsilon^2}, 0)$$
$$Z_{\mathsf{n}}^{(B)} = (\epsilon, 0, \sqrt{1-\epsilon^2})$$

- Both operators have small overlap ϵ with ground state
- Operators are approximately orthogonal

GEVP eigenvalues controlled by first and second excited state (**not** ground state) for $\epsilon \ll e^{t(E_1-E_0)}$

$$\lambda_0^{(AB)} = e^{-(t-t_0)E_1} + O(\epsilon^2)$$
$$\lambda_1^{(AB)} = e^{-(t-t_0)E_2} + O(\epsilon^2)$$

Off-diagonal correlator conversely has perfect ground-state overlap

Lanczos = Prony = …

Algebraic methods for decomposing time series into sum of exponentials known since 1795

Prony and Gaspard (1795)

Applications of Prony's method to LQCD first proposed by Fleming in 2004

Fleming arXiv:hep-lat/0403023 (2004)

Other equivalent implementations possible, e.g. Prony generalized eigenvalue method (PGEVM)

Fischer et al, Eur. Phys. J. A 56, 206 (2020)

Hackett, MW, arXiv:2412.04444

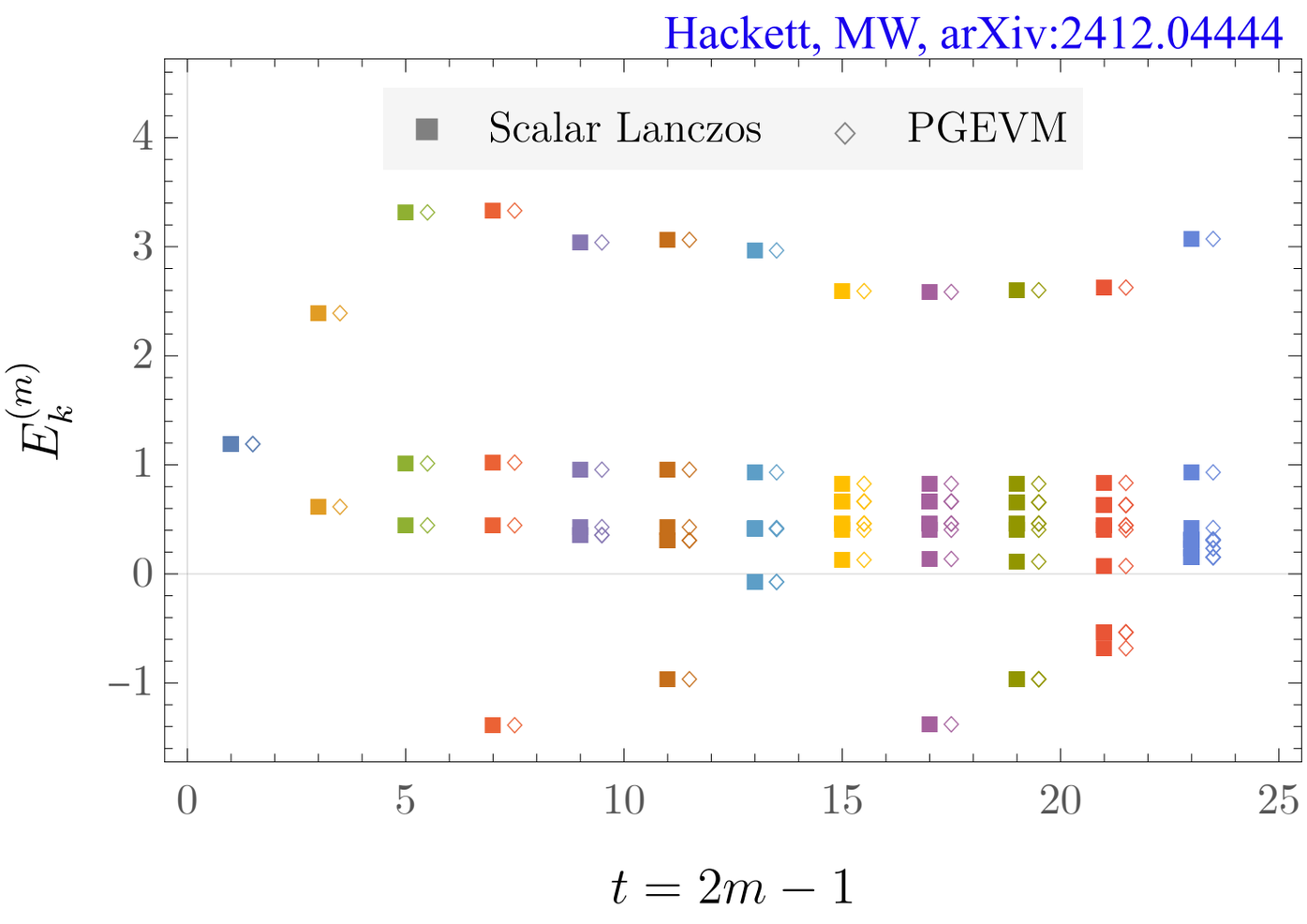

Lanczos and Prony produce identical energy estimators for noisy data

MW, arXiv:2406.20009 Ostmeyer et al, arXiv:2411.14981 Chakraborty et al, arXiv:2412.01900

Rayleigh-Ritz is all you need

One step of block Lanczos = GEVP

Lüscher and Wolff, Nucl. Phys. B 339, 222 (1990)

Block Lanczos is a strict generalization of GEVP

Block Lanczos = Block Prony

Fleming, LATTICE2023

= GPOF

Aubin and Orginos, MENU 2010

Hackett, MW, arXiv:2412.04444

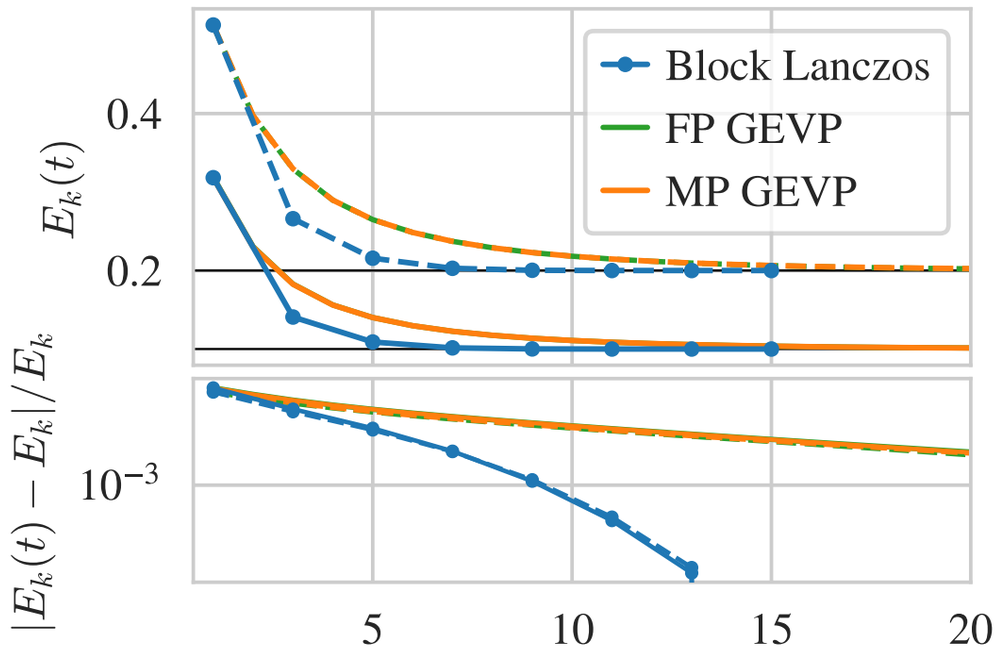

These and more ***coincidences in Krylov space*** between Rayleigh-Ritz methods explored in

Abbot, Fleming, Hackett, Pefkou, MW, arXiv:2401.XX

RR Name	Convergence	Hermiticity	Block	Correlator analysis methods
RR / ORR	Power iteration	Yes / No	No	Effective masses, ratios, etc.
RR / ORR	Power iteration	Yes / No	Yes	GEVP methods
KRR	KPS	Yes	No	Lanczos, Prony, GPOF/PGEVM/TGEVP
BKRR	KPS	Yes	Yes	Block Lanczos, Block Prony, GPOF
OKORR	Oblique KPS	No	No	Oblique Lanczos, Prony, GPOF/PGEVM/TGEVP
OBKORR	Oblique KPS	No	Yes	Oblique block Lanczos, Block Prony, GPOF

TABLE I. Taxonomy of various methods for correlator analysis as they relate to the Rayleigh-Ritz method.

KPS convergence theory

Lanczos converges exponentially faster than power iteration for transfer matrices with small gaps (e.g. for small a)

Kaniel, Mathematics of Computation 20, 369 (1966)

$$\delta = a(E_1 - E_0)$$

Paige, PhD thesis 1971

$$\left|E_0 - E_0^{(m)}\right| \propto e^{-2t\sqrt{\delta}}$$

Lanczos

Saad, SIAM 17 (1980)

$$\left|E_0 - E_0^{\text{eff}}(t)\right| \propto e^{-t\delta}$$

Power iteration

- Convergence benefits largest near continuum limit where $1 \gg \sqrt{\delta} \gg \delta$
- Prony (= Lanczos) has identical convergence, but we didn't know the rate before

Block Lanczos converges exponentially faster than GEVP for transfer matrices with small gaps (e.g. for small a)

$$\delta_r = a(E_r - E_0)$$

Saad, SIAM 17 (1980)

$$\left|E_0 - E_0^{(m)}\right| \propto e^{-2t\sqrt{\delta_r}}$$

Block Lanczos

$$\left|E_0 - E_0^{\text{GEVP}}(t)\right| \propto e^{-t\delta_r}$$

GEVP